Fall 12-2022

Atlantic Surfclam (*Spisula Solidissima*) Population Demographics and Distribution Along the Middle Atlantic Bight

Mauricio González Díaz
Old Dominion University, maugondiaz@gmail.com

Recommended Citation

González Díaz, Mauricio. "Atlantic Surfclam (*Spisula Solidissima*) Population Demographics and Distribution Along the Middle Atlantic Bight" (2022). Master of Science (MS), Thesis, Ocean & Earth Sciences, Old Dominion University, DOI: 10.25777/qkm2-s578
https://digitalcommons.odu.edu/oeas_etds/187

ATLANTIC SURFCLAM (*SPISULA SOLIDISSIMA*) POPULATION DEMOGRAPHICS AND DISTRIBUTION ALONG THE MIDDLE ATLANTIC BIGHT

by

Mauricio González Díaz
B.S. January 2019, Universidad Austral de Chile, Chile

A Thesis Submitted to the Faculty of
Old Dominion University in Partial Fulfillment of the
Requirements for the Degree of

MASTER OF SCIENCE

OCEAN AND EARTH SCIENCES

OLD DOMINION UNIVERSITY
December 2022

Approved by:

John M. Klinck (Director)

Eileen E. Hofmann (Member)

Daphne Munroe (Member)

ABSTRACT

ATLANTIC SURFCLAM (*SPISULA SOLIDISSIMA*) POPULATION DEMOGRAPHICS AND DISTRIBUTION ALONG THE MIDDLE ATLANTIC BIGHT

Mauricio González Díaz
Old Dominion University, 2022
Director: Dr. John M. Klinck

The Atlantic surfclam (*Spisula solidissima*) is a long-lived benthic biomass dominant organism that occurs on the Middle Atlantic Bight (MAB) continental shelf between 10 m and 50 m. Trends in Atlantic surfclam population specific growth and mortality rates were analyzed using four decades of age and length observations obtained from NOAA stock surveys from the 1980s to 2010s in six regions distributed along the MAB. Atlantic surfclam specific growth rates and asymptotic lengths were estimated from the age and length observations using the von Bertalanffy growth model. The analysis showed that the Atlantic surfclam median asymptotic length in the southern regions of the MAB was smaller, 88 mm, relative to asymptotic lengths of 110 mm to 141 mm estimated for the northern survey regions. The asymptotic lengths estimated from observations in the southern-most survey region declined by 35% over the four decades. Constant and age-dependent specific mortality rates were estimated from the age and length observations with the relationship given in Hoenig (1985) and a hyperbolic tangent relationship based on the change in number with age, respectively. The decadal averaged specific mortality rate overall survey regions of 0.20 y^{-1} is consistent with mortality rate estimates from literature, but considerable variability was obtained within and between survey regions. The highest specific mortality rates of 0.18 yr^{-1} to 0.58 yr^{-1}

were associated with the southern survey regions, where the Atlantic surfclam population had age distributions skewed to younger ages. The estimated specific growth and mortality rates were input to a numerical model that simulates the population dynamics of Atlantic surfclams to assess controls on the alongshelf gradient in population density. A comparison of simulated distributions with observed distributions showed that age-dependent mortality is the primary determinant of the Atlantic surfclam population density gradient. The trends in population growth and mortality rates reflect changes in Atlantic surfclams imposed by warming bottom water temperatures. These results have implications for projecting Atlantic surfclam responses to a warming habitat.

To my parents and family: Margarita, Mauricio, Nicolás, and Berni, who have always believed in and supported me in every step on the way.

In loving memory of Zoe Baudissin. Your passion and kindness inspired every person crossing paths with you.

ACKNOWLEDGMENTS

The completion of this work would not have been possible without the guidance of my advisers Dr. John Klinck and Dr. Eileen Hofmann. Their endless patience and support beyond limits made this challenge a great experience, even through these crazy times.

I would also like to thank Dr. Daphne Munroe and Dr. Sarah Borsetti from Rutgers University, whose ideas and encouraging words helped me to gain self-confidence and understand the importance of working with a dedicated and empathic research group.

I am grateful to Dr. Eric Powell, from the University of Southern Mississippi, who provided the data and his fieldwork knowledge on the techniques used to collect the data.

Finally, I would like to thank every member of CCPO who made me feel included and part of this great family. As well as the friends I made in grad school, especially Iliana Flefel and Nicole Buckley, who always provided moral support and an extra brain to explore new ideas.

Funding for this study was provided by the U.S. Department of the Interior, Bureau of Ocean Energy Management, Environmental Studies Program, Washington DC, under contract number M19AC00016.

NOMENCLATURE

DMV	Delmarva Peninsula
GBK	Georges Bank
LI	Long Island
MAB	Middle Atlantic Bight
NEFSC	Northeast Fisheries Science Center
NOAA	National Oceanic and Atmospheric Administration
NJ	New Jersey
SNE	Southern New England
SVA	Southern Virginia

TABLE OF CONTENTS

Page

LIST OF TABLES

Table Page

LIST OF FIGURES

Figure Page

Figure Page

INTRODUCTION

The seven recognized marine ecosystems of the Northwest Atlantic share common oceanographic and ecological features, and each supports a suite of marine organisms, many of which have a long history of commercial exploitation (Link et al. 2011). The key pelagic and benthic species vary across the ecosystems of the Northwest Atlantic. The Middle Atlantic Bight (MAB) region, the portion of the Northwest Atlantic continental shelf system between Cape Hatteras and Nantucket Shoals (Fig. 1), is characterized by a productive benthic ecosystem dominated by the Atlantic surfclam (*Spisula solidissima,* Dillwyn 1817). Historically, this long-lived (∼30 years) benthic biomass dominant extended over the MAB shelf between depths of 10 m to 50 m (Fig. 1, Abbott 1974, Ropes 1978, Cargnelli et al. 1999). The Atlantic surfclam supports a lucrative fishery, with nominal revenues of about $33 million per annum (NEFSC 2017), which constitutes a significant fraction of the MAB commercial fishing industry (McCay et al. 2011).

Atlantic surfclams have an optimal environmental temperature range of 16°C to 22°C (Kim & Powell 2004, Marzec et al. 2010, Munroe et al. 2013, Munroe 2016, Acquafredda et al. 2019). Above the upper thermal limit, Atlantic surfclam filtration is reduced, and respiration is increased, which decreases the scope for growth, eventually producing mortality (Cargnelli et al. 1999, Kim & Powell 2004, Weinberg 2005, Zhang et al. 2015, Hornstein et al. 2018, Acquafredda et al. 2019). The thermal effect on Atlantic surfclam physiology constrains the species to areas of the MAB where bottom water temperatures are within its thermal range (Weinberg 1993, 1998, Weinberg et al. 2002, Acquafredda et al. 2019). The Atlantic surfclam range is, therefore, closely aligned with the distribution of cool bottom water temperatures, especially the Cold Pool (Powell et al. 2020, Friedland et al. 2022) that forms on the MAB continental shelf below the thermocline during spring and summer (Ford et al. 1952, Houghton et al. 1994, Brown et al. 2012, Gawarkiewicz et al. 2012).

The thermal constraint on Atlantic surfclam physiology makes the species vulnerable to climate-related warming of the bottom temperatures that change the distribution of suitable habitats. Warming of MAB bottom temperatures was observed in the 1990s, with higher rates of warming occurring in the southern MAB (Mountain 2003). Subsequent studies confirmed that MAB waters have been warming since the 1970s and that the most significant warming is located in the southern MAB (Jossi & Benway 2003, Wallace et al. 2018). Coincident with this warming, the Atlantic surfclam biomass off the Delmarva Peninsula began to decline, with the most significant decrease occurring along the southern and inshore regions from Delaware Bay southwards (Weinberg et al. 2002, Weinberg 2005). At the same time, Atlantic surfclam abundance increased along the offshore range boundary off New Jersey and inshore of Long Island, resulting in a progressive northward and offshore shift in the MAB Atlantic surfclam population (Weinberg et al. 2002, Weinberg 2005, Timbs et al. 2019). The northward contraction of the Atlantic surfclam range and continuing warming of MAB waters have implications for the commercial fishery (Hennen et al. 2018).

Concurrent with climate-related changes in environmental conditions is the expansion of the development of offshore wind energy on the MAB shelf (Haggett et al. 2020, Methratta 2020). The areas identified for placement of offshore wind energy areas overlap Atlantic surfclam abundance areas that support the commercial fishery (Haggett et al. 2020, Methratta 2020). Fishing within the offshore wind energy areas will be severely curtailed or eliminated, especially for the Atlantic surfclam dredge fishery (Scheld et al. 2022). The impact on fisheries from combined climate-related warming and offshore wind energy development will be species-specific; the Atlantic surfclam and the fishery it supports are at-risk from both. Assessment of the risk exposure for this commercially important species requires an understanding of changes in population demographics and population-specific processes, such as mortality and recruitment, so that these can be used to guide model-based projections of future states. The overall goal of this research is to identify changes in the Atlantic surfclam population demographic and assess the effect of those changes on population distribution. This goal was addressed with research questions designed to evaluate 1) changes in Atlantic surfclam demographic parameters from 1980 to present and 2) the effect of population-specific mortality rate in determining Atlantic surfclam distribution along the MAB. The research questions were addressed with a combined data analysis and modeling approach. Age and shell length (hereafter length) observations from NOAA Northeast Fisheries Science Center (NEFSC) stock surveys of the MAB Atlantic surfclam population done between 1982 and 2019 (NEFSC 2022) were the basis for the analysis of demographic parameters. A numerical model that simulates Atlantic surfclam biomass along the MAB (Munroe et al. 2022) was used to assess the effect of mortality rate on population distribution.

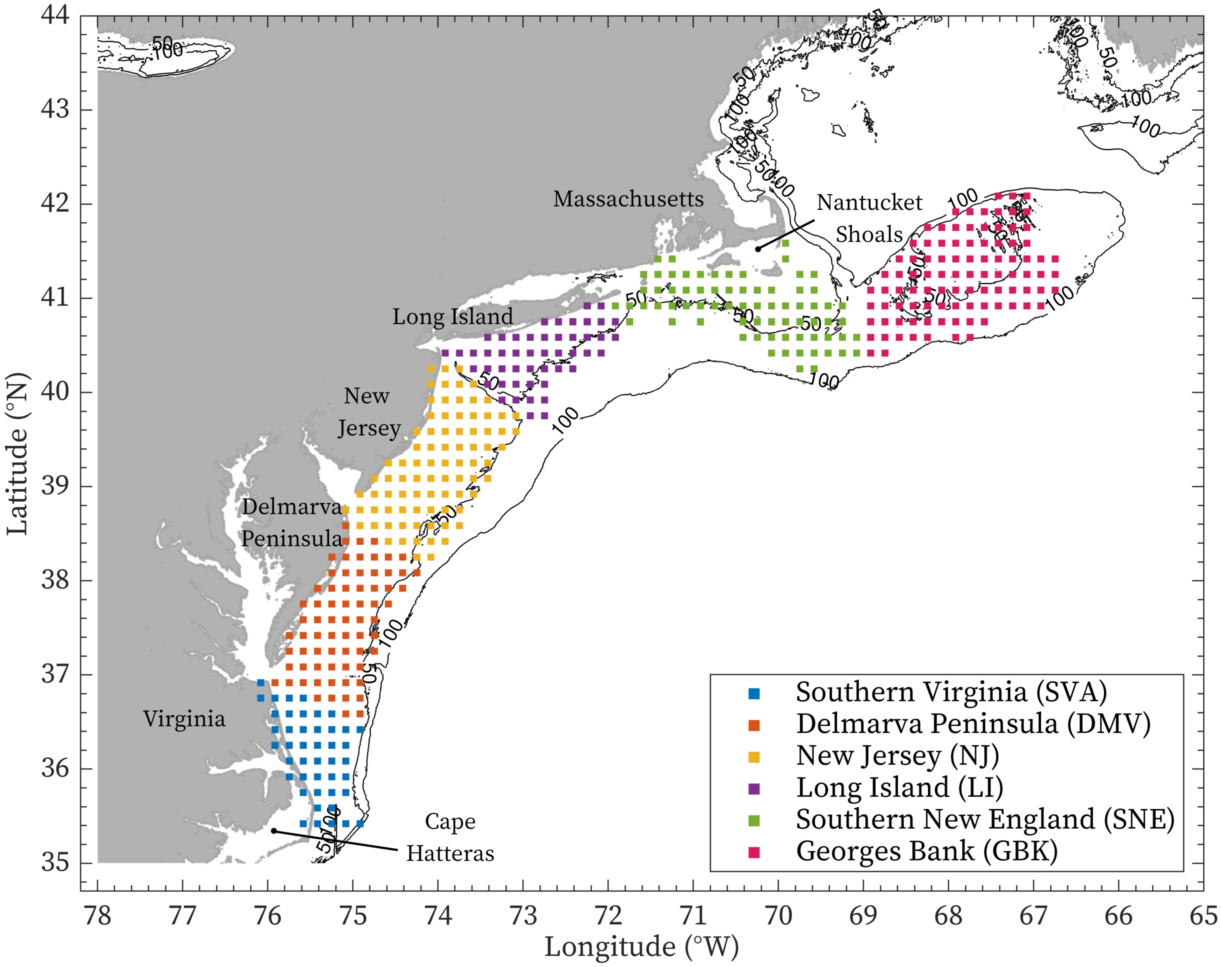

Figure 1. Map of the Middle Atlantic Bight showing the areas (colors) included in the NOAA Northeast Fisheries Science Center Atlantic surfclam survey. The six sub-regions are used to apportion the observations from the Atlantic surfclam survey that are used in this study. The 50 m and 100 m isobaths are indicated.

BACKGROUND

Environmental setting – Middle Atlantic Bight

The circulation over the MAB shelf is predominantly to the south-southwest towards Cape Hatteras (e.g., Beardsley & Winant 1979, Lentz 2008, Levin et al. 2018). The southward flow is driven by inputs from the Labrador Sea, which continue into the MAB (Chapman & Beardsley 1989). The outer MAB shelf presents a shelf-break front that separates the fresher waters (≤34‰) from saltier slope waters (≥35‰) (Linder & Gawarkiewicz 1998). The shelf-break front is variable in space and time and regulates exchange between shelf waters and offshore slope waters, which are influenced by the Gulf Stream and its associated eddies (e.g., Beardsley 1981, Gawarkiewicz et al. 2012, Zhang & Gawarkiewicz 2015).

The waters over the MAB undergo seasonal changes in stratification (Bigelow 1933, Ketchum 1964, Houghton et al. 1982). Intense winter mixing results in a vertically homogeneous water column, which stratifies the following spring and summer as surface waters warm, with the strongest stratification occurring between August and September (Bigelow 1933, Ketchum 1964, Houghton et al. 1982). The combination of the seasonal stratification and the input of cold Labrador Sea water produces a unique hydrographic feature on the MAB shelf. The intense summer stratification and reduced mixing isolate the bottom waters, trapping an extensive pool of cold water, referred to as the Cold Pool (Bigelow 1933, Houghton et al. 1982). This hydrographic feature appears as a band of cold bottom water (at 50 m to 80 m Houghton et al. 1982) with minimum temperatures between 4°C and 12°C (Davis 1979, Gawarkiewicz et al. 2012) that extends from Georges Bank to Cape Hatteras (Bigelow 1933, Ketchum 1964, Beardsley & Winant 1979, Houghton et al. 1982).

Variability in the Cold Pool temperatures results from differences in the deepening of the thermocline (Ketchum 1964), variations in the topography along the shelf (Houghton et al. 1982), the position of the shelf-slope front (Davis 1979, Gangopadhyay et al. 2019, 2020), and variability of the warming of surface waters during the spring (Davis 1979). The Cold Pool remains intact throughout the summer and is eroded in the fall and winter as mixing increases and reduces the vertical temperature gradient.

The Cold Pool forms primarily from the isolation of cold water produced during the winter, but inputs from other sources contribute to its existence. Upstream sources from Georges Bank contribute to the maintenance of the Cold Pool (Chen et al. 2018). Variations in the volume, salinity, and temperature of the Cold Pool have been associated with an inflow of Gulf of Maine waters (Mountain 2003, Andres et al. 2013), variability in Labrador Sea inputs (Mountain 1991), and regime shift in the formation and intrusion of warm-core rings from the Gulf Stream to the shelf break (Gangopadhyay et al. 2019, 2020, Friedland et al. 2022).

Warming of the Cold Pool has occurred over the past 4 to 5 decades as evidenced by warming of 1°C in the inner shelf (Jossi & Benway 2003) and 2°C above the average temperatures close to the shelf-slope (Mountain 2003) during the winter. This warming has been attributed to fluctuations in the atmospheric heat flux (Shearman & Lentz 2010, Lentz 2017), warmer and longer summers (Friedland & Hare 2007, Chen et al. 2014, Friedland et al. 2020, 2022), and interactions between the slope waters and continental shelf waters (Kang & Curchitser 2013, Lentz 2017). For the latter, an unusual warming event in 2011 was attributed to interactions between slope waters and the Gulf Stream, which introduced warmer water onto the shelf (Gawarkiewicz et al. 2012). This event corresponded to a regime shift in the generation and intrusion of warm-core rings from the Gulf Stream into the shelf break, increasing the number of warm-core rings from 18 (1980 – 1990) to

33 warm-core rings (2000 – 2017) (Gangopadhyay et al. 2019, 2020).

Atlantic Surfclam Ecology

The Atlantic surfclam is biomass dominant in the benthic environment of the MAB (Cargnelli et al. 1999) and is supported by a habitat within the optimal range for the species. Also, the high primary production of the shelf (O'Reilly & Busch 1984, Yoder et al. 2002, Xu et al. 2011, 2020) and resuspended benthic material (Munroe et al. 2013) provide food resources that are adequate to support Atlantic surfclam growth.

Atlantic surfclams have a biannual reproductive cycle characterized by two spawning events, a major mid-year and a minor late-year spawning (Ropes 1968). The planktonic larvae remain in the water column for about 35 days (Zhang et al. 2015). Vertical migration helps to retain the larvae in the inner-shelf region where the temperature is favorable for their growth and development (Zhang et al. 2015). Along-shelf larval transport, which is predominant to the south, connects the Atlantic surfclam population along the MAB (Zhang et al. 2016). The exception is the population associated with Georges Bank, which is relatively isolated by the closed circulation of this region (Zhang et al. 2015, 2016). Patterns of recruitment rates into the Atlantic surfclam population indicates higher recruitment off New Jersey ($\sim$2.20 clams yr^{-1} over a standardized area of 423 m^2, Weinberg 1999), in contrast with southern MAB locations, which experience considerably lower recruitment rates ($\sim$0.65 clams yr^{-1} over a standardized area of 423 m^2, Loesch & Ropes 1977, Weinberg 1999).

Atlantic surfclam growth rates vary along the MAB. Specific growth rates were estimated to be slowest for southern MAB locations ($\sim$0.17 yr^{-1}, Weinberg & Helser 1996, Weinberg 1999), gradually increasing in central locations ($\sim$0.25 yr^{-1}, Weinberg & Helser 1996, Weinberg 1999).

The specific growth rates are sufficient for Atlantic surfclams to reach 80 mm in two years, and recruit to the fishery (Loosanoff & Davis 1963, Loesch & Ropes 1977).

Atlantic surfclam populations experience density-dependent competition at densities higher than 0.14 clams m^{-2} (Weinberg 1998), and locations with high densities have higher predation rates (Ropes 1968, Quijon et al. 2007). Density-dependent control and predation mortality contribute to spatial heterogeneity in Atlantic surfclam distribution by reducing regional differences produced by recruitment variability (Quijon et al. 2007). Atlantic surfclam size contributes to the effects of competition and mortality. Small (<50 mm) Atlantic surfclams are more sensitive to competition (Weinberg 1999) and predation (Weinberg 1998). Adult Atlantic surfclams (>70 mm) mortality is mainly related to fisheries (Weinberg 1999), predation (Quijon et al. 2007), and temperature variations (Weinberg et al. 2002).

Effects of Warming on Atlantic Surfclam

The temperature range that supports adult Atlantic surfclam growth is 16°C to 22°C (Kim & Powell 2004, Marzec et al. 2010, Munroe et al. 2013, Munroe 2016, Acquafredda et al. 2019). Higher temperatures are lethal for larvae, juveniles (Snelgrove et al. 1998, Zhang et al. 2015, Acquafredda et al. 2019), and adults (Loosanoff & Davis 1963, Savage 1976, Kim & Powell 2004). Metabolic rates of Atlantic surfclam increase as temperature increases (DeFur & Mangum 1979, Freitas et al. 2009). Atlantic surfclam respiration rates are higher than the average for other bivalves, as suggested by burrowing rates measured on the North Atlantic continental shelf (Savage 1976, Alexander et al. 1993). Respiration rate scales as the cube of the length (Powell & Stanton 1985, Freitas et al. 2009, Powell et al. 2016), whereas ingestion scales as the square of the length (Powell et al. 1992, Hofmann et al. 2006, van der Meer 2006). As a result, Atlantic surfclams experiencing warming are unable to ingest sufficient food to meet respiration demands, and the animal starves (Marzec et al. 2010). The already high respiration demands of Atlantic surfclam (Savage 1976, Alexander et al. 1993, Munroe et al. 2013) combined with small changes in temperature can have significant deleterious effects on the population (Weinberg et al. 2002, Narváez et al. 2015, Munroe et al. 2016).

The physiological constraint imposed by temperature has been suggested as the cause for the observed reduction of biomass in the Delmarva Peninsula region of the MAB in the late 1990s to early 2000s (Weinberg et al. 2002). Inshore waters reached temperatures in the summer that were lethal for Atlantic surfclams (O'Beirn et al. 1997) and produced poor physiological conditions, resulting in high mortalities in shallow waters of the Delmarva Peninsula region (Weinberg et al. 2002), and displacement of the population depths of 25 – 35 m to offshore waters of 35 – 46 m (Weinberg 2005). A subsequent study by Marzec et al. (2010) showed that adult Atlantic surfclams at the edge of the MAB shelf had poorer condition relative to those in the center of the Cold Pool, which was attributed to warmer temperature fluctuations and reduced nutrients at the shelf edge. Simulations of Atlantic surfclam growth showed that populations located along the outer MAB were more frequently affected by warm water from the Gulf Stream and shelf slope, which decreased condition and increased mortality (Narváez et al. 2015). An increase in bottom water temperatures of 2°C above the average produced a 2 – 9 % in mortality due to thermal stress (Narváez et al. 2015) and resulted in a decrease of 10 % in maximum length along the MAB (Munroe et al. 2016).

METHODS

Stock Survey Data

The NOAA NEFSC Atlantic surfclam stock surveys encompass the MAB shelf region from offshore Southern Virginia to Georges Bank (Fig. 1) and are designed to overlap with the primary Atlantic surfclam fishery areas (Weinberg 2005, NEFSC 2017). The survey areas are approximately the same for each survey region (NEFSC 2017). In 2012, the NEFSC modified the survey protocol by changing the dredge, and hence dredge efficiency, used for the survey. The stock surveys from 2012 to present used the different dredge.

Atlantic surfclam surveys in the six survey regions used in this study were done from 1982 to 2019 at intervals of about 3 years (NEFSC 2017, 2022, Table 1), with minor differences in the timing of the surveys. For example, the Southern Virginia region was surveyed less frequently during the 1990s and early 2000s, and the Southern New England region was surveyed more frequently after 2012 (Table 1).

For each survey region, the stock survey data provided Atlantic surfclam age and length measurements as well as counts of individuals (NEFSC 1995, 2017, 2022). The age and length data were binned by survey region (Fig. 2A) and by decade (Fig. 2B). The binning provided good data coverage across regions and decades and reduced variability associated with limited measurements in some regions (Table 1). The age and length data are not affected by the change in survey protocol in 2012, which allows the stock survey data from 2012 to 2019 to be included, providing almost four decades of observations (Fig. 2, Table 1).

The counts of individuals were used to calculate Atlantic surfclam density for the 1990s to 2010s for each survey region, with the exception of Georges Bank, for which no density data are available for any decade.

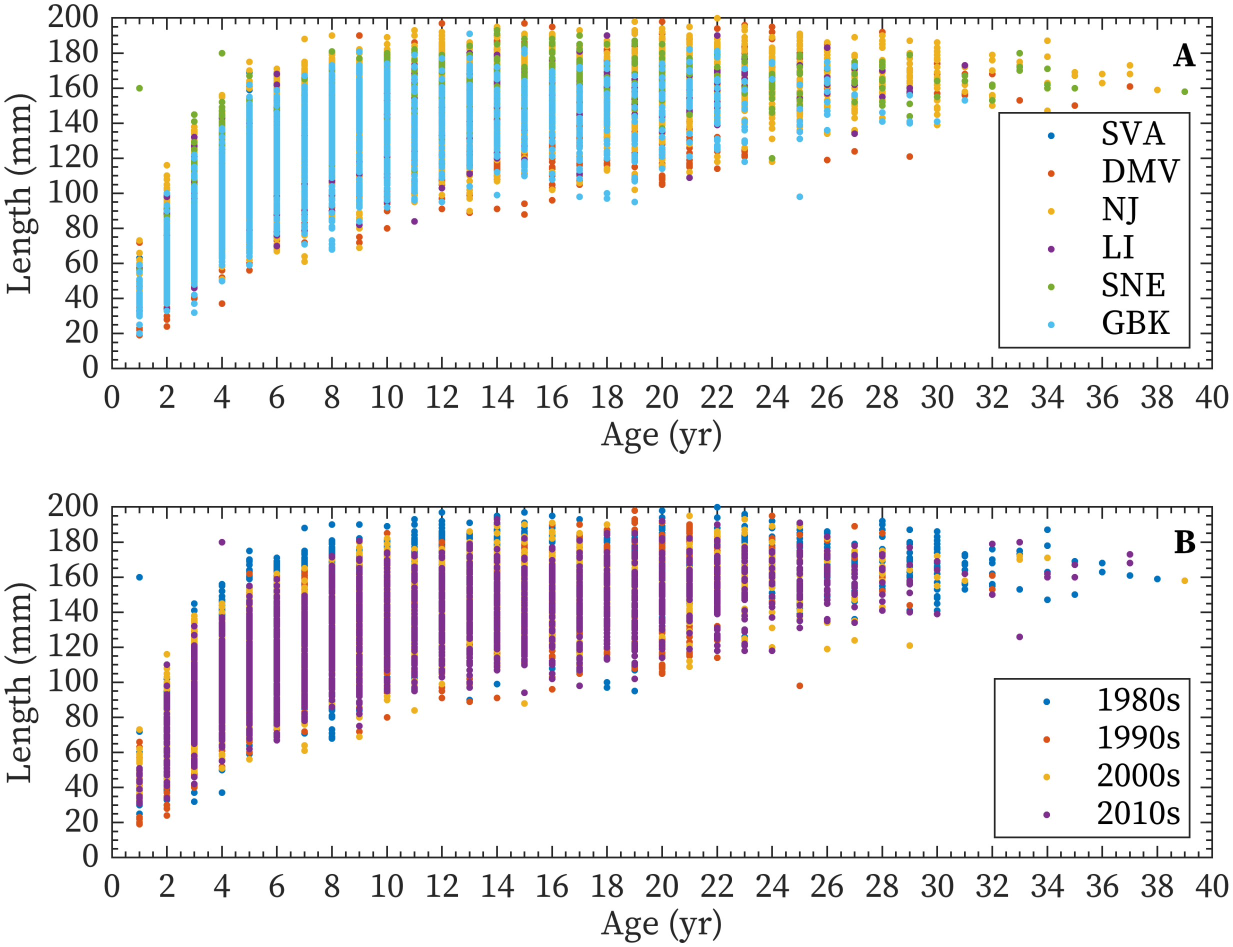

Figure 2. Age (yr) and length (mm) data obtained from the NEFSC Atlantic surfclam stock surveys from 1982 to 2019 binned by (A) survey region and (B) decade. The survey region locations and definitions are shown in Figure 1.

TABLE 1.
NEFSC survey regions (south to north), years surveyed, and number of observations per decade. The survey regions are shown in Figure 1.

Region	Years Surveyed	Number of Observations
Southern Virginia	1982, 1983, 1986, 1989	185
	1992	8
	2002, 2005	29
	2011, 2012, 2015, 2018	70
Delmarva Peninsula	1982, 1983, 1986, 1989	2089
	1992, 1994, 1997, 1999	1560
	2002, 2005, 2008	986
	2011, 2012, 2015, 2018	385
New Jersey	1982, 1983, 1986, 1989	3726
	1992, 1994, 1997, 1999	1468
	2002, 2005, 2008	1865
	2011, 2012, 2015, 2018	1151
Long Island	1982, 1983, 1986, 1989	126
	1992, 1999	69
	2002, 2005, 2008	271
	2011, 2012, 2015, 2018	373
Southern New England	1982, 1983, 1986, 1989	622
	1992, 1999	104
	2002, 2005, 2008	98
	2011, 2013, 2014, 2015, 2016, 2018	99
Georges Bank	1982, 1984, 1986, 1989	1111
	1992, 1997, 1999	539
	2002, 2008	264
	2011, 2013, 2014, 2016, 2019	642

Demographic Parameters Estimation

Growth Rate

Atlantic surfclam growth rates were estimated from the age (a) and length (L) observations using the von Bertalanffy relationship (von Bertalanffy 1938) that gives length at age, $L(a)$, as

$$L(a) = L_\infty(1 - e^{-k(a-a_0)}) \tag{1}$$

where L_∞ is the asymptotic length (mm), k is the instantaneous specific growth rate (yr^{-1}), and a_0 is the initial age (yr). The von Bertalanffy equation was fit to the binned age and length observations from each region and each decade using a nonlinear curve fitting routine (*nlinfit*, MATLAB, Seber & Wild. 2003). The curve fits yielded estimates of the instantaneous specific growth rate, k, and asymptotic length, L_∞. A specific growth rate, g, for a given length, L, is then obtained from

$$g = k(L_\infty - L) \tag{2}$$

which is input to the Atlantic surfclam population model (see section *Model Implementation* for details).

The von Bertalanffy growth curves obtained using the age and length observations from the New Jersey survey region, which is intermediate between the southern and northern survey regions, provide examples of variability in k and L_∞ in the 1980s, 1990s, 2000s, and 2010s (Fig. 3). The growth curves for the other five survey regions are provided in the Supplemental materials (Fig. A.1 – A.5). The estimated k and L_∞ parameters for the six survey regions for the four decades are summarized in Table 2 (more details in Table B.1).

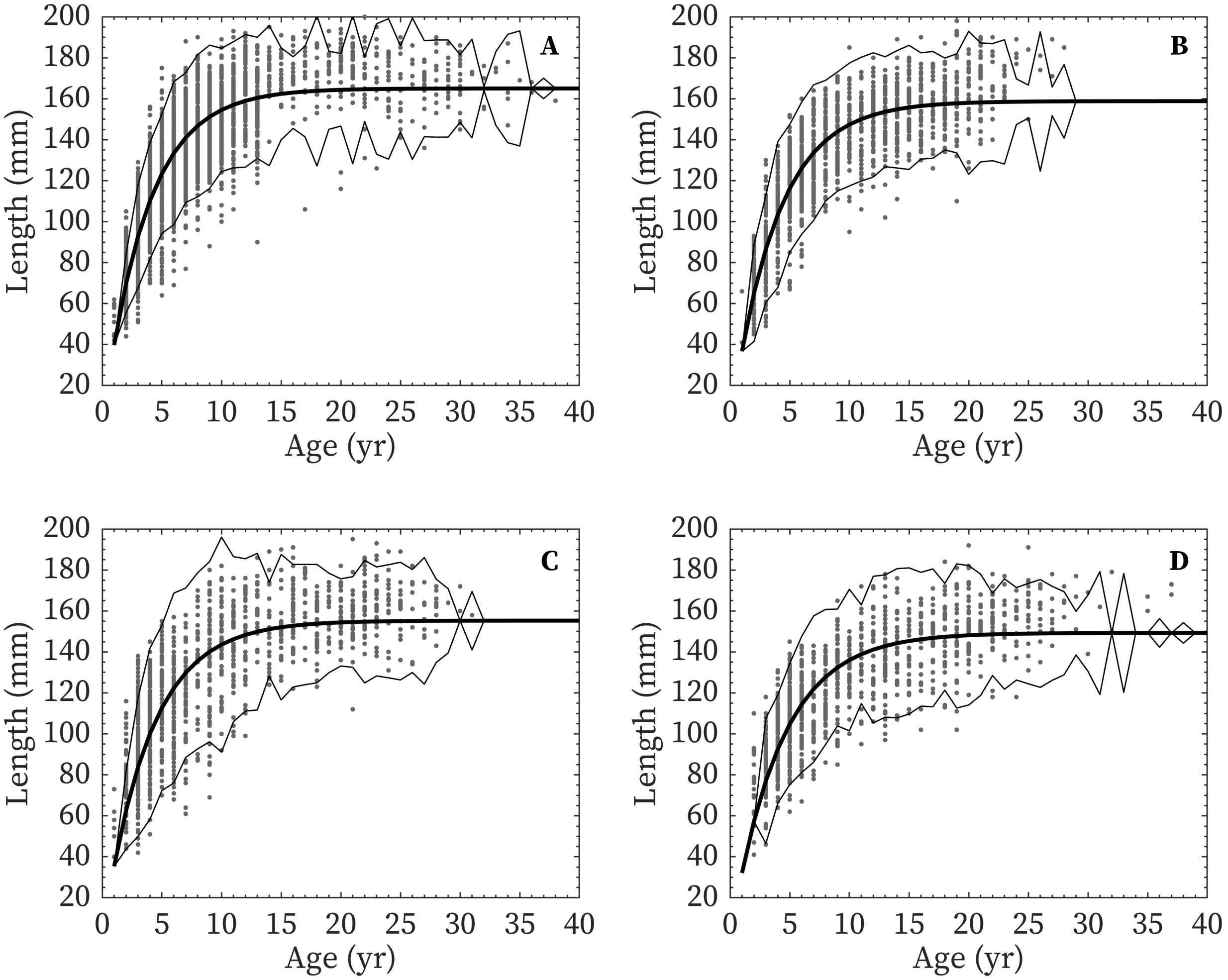

Figure 3. Atlantic surfclam age (yr) versus length (mm) observations (grey dots) obtained from the New Jersey survey region for (A) 1980s, (B) 1990s, (C) 2000s, and (D) 2010s. The growth curve (heavy line) and standard deviation (2σ, thin line) obtained from the von Bertalanffy equation fit to the observations for each decade is shown. All curve fits are significant ($p < 0.001$) with r^2 values of 0.74 for the 1980s, 0.75 for the 1990s, 0.62 for the 2000s, and 0.65 for the 2010s.

TABLE 2.
Atlantic surfclam specific growth rate (yr^{-1}), asymptotic length (mm), average length (mm), and standard deviation (SD) estimated from the age and length observations for each survey location and each decade. The survey regions are listed from south to north along the MAB shelf. The survey regions are shown in Figure 1.

Survey Region	Decade	Specific Growth Rate (yr^{-1})	Asymptotic Length (mm)	Average Length (mm ±SD)
Southern Virginia	1980s	0.34	153	124 (±30)
	1990s	0.37	143	88 (±32)
	2000s	0.38	131	71 (±33)
	2010s	0.68	105	89 (±19)
Delmarva Peninsula	1980s	0.23	168	127 (±32)
	1990s	0.26	142	114 (±30)
	2000s	0.29	141	113 (±32)
	2010s	0.32	126	103 (±26)
New Jersey	1980s	0.27	165	128 (±31)
	1990s	0.26	159	131 (±31)
	2000s	0.26	155	126 (±33)
	2010s	0.24	149	123 (±28)
Long Island	1980s	0.25	163	140 (±31)
	1990s	0.34	159	128 (±30)
	2000s	0.34	155	124 (±34)
	2010s	0.28	153	128 (±29)
Southern New England	1980s	0.28	165	141 (±30)
	1990s	0.24	164	115 (±42)
	2000s	0.25	167	142 (±34)
	2010s	0.25	166	146 (±30)
Georges Bank	1980s	0.24	148	102 (±35)
	1990s	0.27	146	106 (±32)
	2000s	0.28	144	114 (±32)
	2010s	0.29	149	131 (±25)

Mortality Rate – Constant Rate

The age and length observations from the stock surveys were used to construct an age-frequency distribution for each survey region in each decade. The age-frequency distribution was used to estimate a constant specific mortality, $M_{constant}$, for each survey region for each decade from the relationship given in Hoenig (1983) and suggested by Hewitt & Hoenig (2005), which was derived using observations from several species, including bivalves. This relationship assumes that the specific mortality rate decreases with increasing age (yr) and is expressed as a negative logarithmic relationship of the form

$$ln(M_{constant}) = a + b\, ln(a_{max}) \tag{3}$$

where a (1.23, number) and b (-0.832, number yr^{-1}) are the constants given in Hoenig (1983) for mollusks, and a_{max} (yr) is the population maximum age.

Equation (3) was used with the Atlantic surfclam age-frequency observations for each survey region for each decade to obtain estimates of specific mortality rates. The maximum age and specific mortality rate estimated using the observations from the survey regions for the 1980s, 1990s, 2000s, and 2010s are shown in Table 3.

TABLE 3.

Atlantic surfclam specific constant mortality rate (yr^{-1}) estimated from the age and length observations using equation (3) for each survey location and each decade. The survey regions are listed from south to north along the MAB shelf. The survey regions are shown in Figure 1.

Survey Region	Decade	Maximum Age (yr)	Constant Mortality Rate (yr^{-1})
Southern Virginia	1980s	25	0.18
	1990s	11	0.38
	2000s	7	0.58
	2010s	8	0.52
Delmarva Peninsula	1980s	36	0.12
	1990s	23	0.19
	2000s	28	0.16
	2010s	23	0.19
New Jersey	1980s	37	0.12
	1990s	27	0.16
	2000s	30	0.15
	2010s	36	0.12
Long Island	1980s	30	0.15
	1990s	18	0.24
	2000s	24	0.18
	2010s	28	0.16
Southern New England	1980s	31	0.14
	1990s	31	0.14
	2000s	38	0.12
	2010s	33	0.13
Georges Bank	1980s	30	0.15
	1990s	27	0.16
	2000s	24	0.18
	2010s	28	0.16

Mortality Rate – Age-Dependent Rate

Inspection of the Atlantic surfclam age-frequency distributions suggested that the population mortality rate is not linear across ages. For example, the age-frequency distribution shown for the New Jersey survey region (Fig. 4) shows a decline in number for about the first 10 years, a plateau in number at the ages of about 10 to 20 years old, and a decrease in the number of older ages. This pattern suggests that Atlantic surfclam populations experience large recruitment events with high mortality for young ages, a stable population at mid-age, and rapid mortality in old age (senescence). Therefore, a relationship that is based on the change in the number of animals per age, $N(a)$, of the form

$$\begin{aligned} N(a) = N_0 \, + \, (\, N_1 \, - \, N_0 \,)\, tanh(\frac{a}{a_1}) - \, (\, N_1 \, - \, dN_1 \, * a_{max} \,) \\ 0.5 \, (\, 1 \, + \, tanh(\frac{a - a_m}{a_r}) \,) + \, aM_{base} \end{aligned} \tag{4}$$

was fit to the age-frequency observations. The change relative to an initial number, N_0, is estimated by fitting two hyperbolic tangents, $tanh$, that represent the change in the number of animals per age, $tanh(\frac{a}{a_1})$ and $tanh(\frac{a-a_m}{a_r})$ where a is the animal age (yr), a_1 is the range that determines the transition from high mortality to a plateau, N_1 is the number at the beginning of the plateau, dN_1 is a small decline in number, a_{max} is maximum age, a_m is the age at which mortality rate is half of the maximum mortality rate, a_r is the range that determines if mortality is closer to zero or its maximum value, and M_{base} is the average base linear mortality.

Equation (4) was fit to the Atlantic surfclam age-frequency observations for each survey region for each decade, except for the Southern Virginia survey region, using a nonlinear curve fitting routine ($nlinfit$, MATLAB, Seber & Wild. 2003) to obtain an age-dependent estimate of specific mortality rate. The Atlantic surfclams in the Southern Virginia survey region were smaller and, as a result, were younger ages (Appendices, Fig. C.1). As a result, the plateau and increase in mortality at an older age were not represented in the age and length observations. This combination did not allow the successful application of Equation (5) to the age and length observations from the Southern Virginia region.

The fit of equation (4) using the observations from the New Jersey survey region for the 1980s, 1990s, 2000s, and 2010s are shown in Figure 4. The age-dependent mortality relationships for the other five survey regions are shown in the Supplemental materials (Fig. C.2 – C.5). The coefficient values obtained from the curve fits for each of the five survey regions where Equation (4) was applied and the four decades, together with statistics values, are given in the Appendices (Table D.1).

Thus, age-dependent mortality, $M_{age-dependent}$, is estimated by differentiation of the equation (4) for each age, giving

$$\begin{aligned} M_{age-dependent} = -\frac{1}{N}\,((N_1 - N_0)\; sech^2\,(\frac{a}{a_1})\;\frac{1}{a_1}\;0.5\;(N_1 - dN_1 a_{max}) \\ sech^2\,(\frac{a-a_m}{a_r})\frac{1}{a_r}\; - M_{base}) \end{aligned} \tag{5}$$

in which the parameters used correspond to the previously estimated from fitting equation (4) to the observations. Mortality was normalized based on the number of individuals present at each age, $-\frac{1}{N}$. A summary of the calculated age-dependent specific mortality rates is found in Table 4.

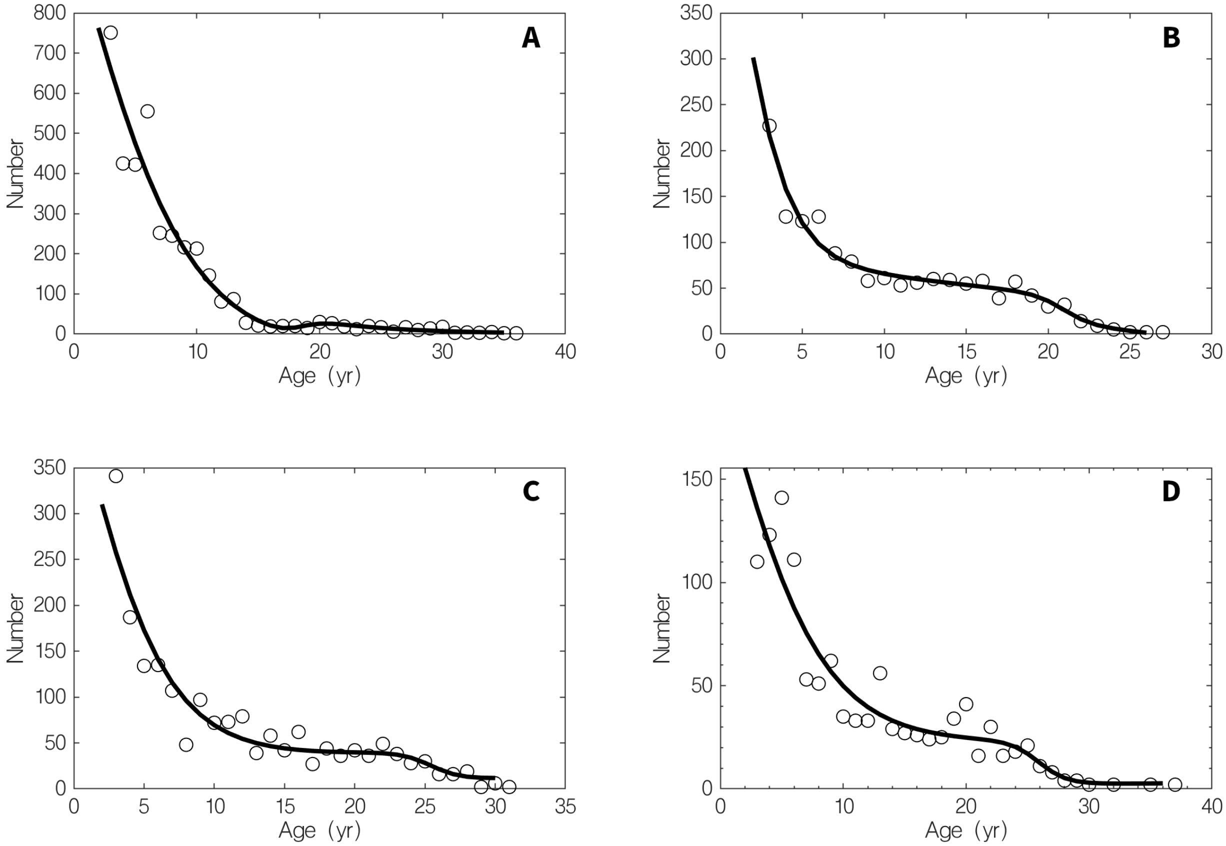

Figure 4. Age (yr) versus number of Atlantic surfclam observations in each age category (circles) obtained from the stock surveys in the New Jersey region for (A) 1980s, (B) 1990s, (C) 2000s, and (D) 2010s. The mortality curve (solid line) obtained from the fit of equation (4) is shown. All curve fits are significant ($p < 0.001$) with r^2 values of 0.93 for the 1980s, 0.95 for the 1990s, 0.87 for the 2000s and 0.85 for the 2010s.

TABLE 4.

Average age-dependent mortality rates (yr^{-1}) estimated from the Atlantic surfclam age and length observations using Equation (4) for each survey location and each decade. The age and length data from the Southern Virginia region did not allow application of the Equation (4). The survey regions are listed from south to north along the MAB shelf. The survey regions are shown in Figure 1. The parameter values obtained for Equation (4) from the non-linear curve fits for the five survey regions where Equation (4) was applied are given in Table D.1.

Survey Region	Decade	Average Age-Dependent Mortality (yr^{-1} ±SD)
Southern Virginia	1980s	–
	1990s	–
	2000s	–
	2010s	–
Delmarva Peninsula	1980s	0.15 ±0.02
	1990s	0.17 ±0.06
	2000s	0.14 ±0.07
	2010s	0.16 ±0.06
New Jersey	1980s	0.18 ±0.04
	1990s	0.18 ±0.06
	2000s	0.15 ±0.04
	2010s	0.14 ±0.06
Long Island	1980s	0.17 ±0.08
	1990s	0.18 ±0.03
	2000s	0.15 ±0.08
	2010s	0.08 ±0.03
Southern New England	1980s	0.14 ±0.06
	1990s	0.17 ±0.13
	2000s	0.16 ±0.09
	2010s	0.10 ±0.06
Georges Bank	1980s	0.20 ±0.06
	1990s	0.12 ±0.09
	2000s	0.17 ±0.08
	2010s	0.12 ±0.09

Atlantic Surfclam Population Model

Model Structure

The growth and mortality rates estimated from the Atlantic surfclam survey observations were input to a numerical model that simulates Atlantic surfclam biomass on the MAB shelf (details in Munroe et al. 2022). The population model simulates Atlantic surfclam biomass using 18 evenly distributed (10 mm intervals) size classes, with the smallest size class set at 20 mm and the largest size class set at 200 mm (Fig. 5). Atlantic surfclam gains and losses from a size class are determined by the growth and mortality rates, respectively. New individuals, provided by the reproductive portion of the population, recruit into the 20 mm size class (Fig. 5).

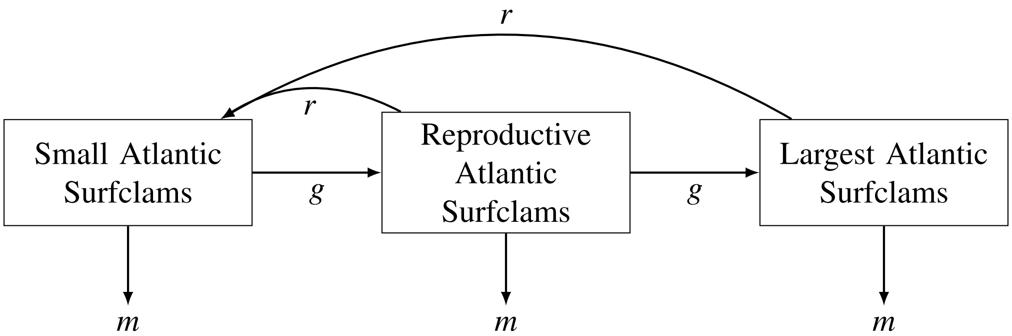

Figure 5. Conceptual diagram for the Atlantic surfclam population dynamics model. Gains and losses from each size class are determined by the growth (*g*) and mortality rates (*m*). Recruitment into the smallest size class is from the reproductive portion of the population (*r*).

The change in Atlantic surfclam numbers in the first size class (N_1) over time (t) is given by

$$\frac{dN_1}{dt} = r - g_1 N_1 - m_1 N_1 \tag{6}$$

where the terms represent recruitment (r) of new individuals and loss from the size class by a size-dependent growth rate (g_1) to the next larger size class and mortality (m), respectively. The change in Atlantic surfclam numbers in all other size classes, N_i, is given by

$$\frac{dN_i}{dt} = g_{i-1} N_{i-1} - g_i N_i - m_i N_i \tag{7}$$

where the terms represent gains from growth from the smaller size class, N_{i-1}, and losses from growth into the next largest size class, N_i, and mortality, respectively. Growth rate is size-dependent.

The recruitment rate, r, is calculated at the end of each simulation year, and follows Beverton & Holt (1993) recruitment dynamics, given by

$$r = \frac{R_A B}{R_B + B} \tag{8}$$

where r is the individuals that recruit into the first size class, B is the total biomass over the whole biological area, R_A and R_B are parameters that follow the Beverton-Holt recruitment dynamics, calculated as

$$R_A = \frac{4(steepness * targetBiomass)}{5 * steepness - 1} \tag{9}$$

and

$$R_B = \frac{(1 - steepness) * targetBiomass}{5 * steepness - 1} \tag{10}$$

where $steepness$ was set as 0.8, following Myers et al. (1999) and O'Leary et al. (2011). The target biomass ($targetBiomass$) was estimated by using a target density of 0.1 clams m^{-2}, calculated from the survey observations, and multiplied by the total biological area.

The size-dependent growth rate, g_i, was determined from equation (1) using the length at the boundary of the discrete size classes and the instantaneous specific growth rate (k) obtained from the fits to the von Bertalanffy equation. Simulations were implemented using a constant mortality rate and an age-dependent mortality rate to assess the effect of different mortality stresses on Atlantic surfclam distribution.

Model Implementation

The Atlantic surfclam population model given by Equations (6) and (7) was solved numerically using a positive-definite advection transport algorithm (MPDATA, Smolarkiewicz & Margolin 1998), which is a flux corrective scheme that allows movement between size classes using estimates of rates at the center of the distribution of each size class. Simulations used time steps of 0.05 years and were run for 100 years to allow the model to reach a stable population. Growth and mortality are calculated at each time step for each size class, whereas recruitment is calculated once per year.

The Atlantic surfclam population model was implemented in a model domain that extends from Georges Bank to Chesapeake Bay and consists of $10'$ latitude by $10'$ longitude squares (ten-minute squares). The model grid is consistent with the survey region used for the Atlantic surfclam stock assessment along the MAB (NEFSC 2017). The region of the MAB that supports Atlantic surfclams, the biological habitat, was defined using bathymetric ranges that are known to constrain the population (10 m – 50 m, Ropes 1968, Abbott 1974) and was imposed on the model domain.

Recruits were distributed throughout the biological habitat using a normal random distribution ($mean = 1$, $std = 0.3$), which is generated when recruitment is calculated.

Model Accuracy and Precision

The model performance was evaluated by comparing simulated Atlantic surfclam densities with densities estimated from the individual counts obtained from the survey. The metrics used to assess model performance were the Root Mean Square Error (RMSE) and Bias in simulated and observed densities, and precision of the simulated and observed densities.

The RMSE, which is the standard deviation of the residuals, is calculated as

$$RMSE = \sqrt{\frac{1}{N}\sum_{i=1}^{n}(X_{model} - X_{obs})^2} \tag{11}$$

where N is the number of ten-minute squares per survey region, X_{model} is the simulated Atlantic surfclam density (number m^{-2}) for a specific ten-minute square, and X_{obs} is the density estimated from observations (number m^{-2}) for the same ten-minute square. This RMSE assesses the overall closeness of the simulated and observed Atlantic surfclam densities.

However, RMSE does not give information about overestimation (or underestimation). The bias of the simulated densities relative to observed densities indicates if differences are from a mismatch over the entire model domain or the result of a few individual ten-minute squares, i.e., outliers.

Thus, the model bias was calculated as

$$Bias = \frac{1}{N}\sum_{i=1}^{n}(X_{model} - X_{obs}) \tag{12}$$

A near-zero bias value indicates that the centroid (or arithmetic mean) of the simulated values matches the centroid of the observations. The RMSE and Bias have the same units as the simulated and observed densities.

The precision of the simulated value was determined using the ratio of the standard deviation of the model, σ_{model}, to the standard deviation of the observations, σ_{obs}, as:

$$P_{\sigma,ratio} = \frac{\sigma_{model}}{\sigma_{obs}} \tag{13}$$

A near-one $P_{\sigma,ratio}$ value indicates similarity in the standard deviations of the simulated and observed values.

RESULTS

Demographic Parameter Analysis

Specific Growth Rate

The specific growth rates estimated from the Atlantic surfclam age and length observations vary within and across survey regions (Table 2, Fig. 6A). The largest growth rates occurred in the Southern Virginia survey region, with a particularly high rate (0.68 yr^{-1}) found in the 2010s. The lowest rate (0.23 yr^{-1}) occurred in the Delmarva Peninsula survey region in the 1980s. Growth rates variability did not show a consistent pattern or trend, with the exception of the Delmarva Peninsula survey region, which had increasing growth rates over the four decades (Table 2, Fig. 6A). Growth rates from the Southern New England and New Jersey survey regions were the least variable over the four decades, with only about a 20% change between the largest and smallest rates. The specific growth rate from the Southern Virginia survey region showed the largest variability over the four decades (Table 5, Fig. 6).

Asymptotic length estimated from the Atlantic surfclam age and length observations also showed within and across survey regions variability (Table 2, Fig. 6B). In Southern Virginia, asymptotic length decreased by about 35% over the four decades. In contrast, asymptotic length in the New Jersey, Long Island, and Southern New England survey regions remained relatively constant over the four decades (Table 2). The average asymptotic length for Atlantic surfclams increased from Southern Virginia to New Jersey over the four decades (Fig. 6B). From New Jersey to Southern New England, asymptotic length was relatively constant at about 160 mm and showed little variability over the four decades (Table 2, Fig. 6B). The asymptotic length associated with

Atlantic surfclams in the Georges Bank survey region was about 145 mm, with an average population length of about 110 mm, around 30% smaller than the populations in the mid and northern MAB survey regions. The asymptotic length estimated for the Southern Virginia survey region showed the most variability (Table 5, Fig. 6B).

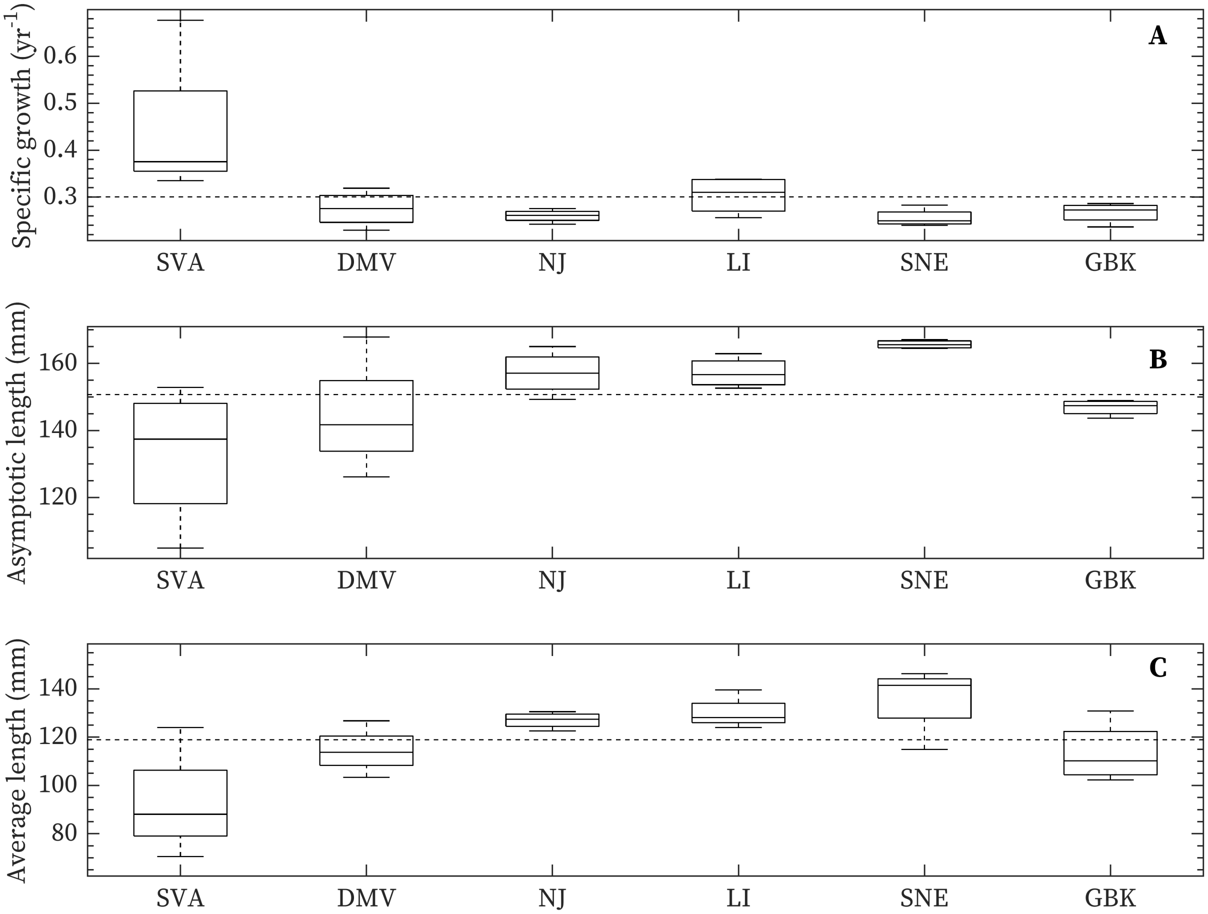

Figure 6. Range of Atlantic surfclam (A) specific growth rate (yr^{-1}), (B) asymptotic length (mm), and (C) average length obtained from the age and length observations for each survey region for the four decades. The decadal median (solid line), maximum and minimum (vertical lines) for each survey region, and the overall average of the MAB (dotted line) are shown. The survey regions are ordered from south to north along the MAB (see Fig. 1) and defined as: Southern Virginia (SVA), Delmarva Peninsula (DMV), New Jersey (NJ), Long Island (LI), Southern New England (SNE), and Georges Bank (GBK).

TABLE 5.
Summary of the maximum, minimum, and median specific growth rate (yr^{-1}), asymptotic length (mm), and average length (mm) estimated from the Atlantic surfclam age and length observations for each survey region and each decade. The difference between the 0.25 and 0.75 quantiles indicates the variability of the data.

	Survey Region	Maximum	Minimum	Median	Quantiles (0.25 — 0.75)
Specific Growth Rate (yr^{-1})	SVA	0.68	0.34	0.38	0.35—0.53
	DMV	0.32	0.23	0.28	0.25—0.30
	NJ	0.28	0.24	0.26	0.25—0.27
	LI	0.34	0.26	0.31	0.27—0.34
	SNE	0.28	0.24	0.25	0.24—0.27
	GBK	0.29	0.24	0.27	0.25—0.28
Asymptotic Length (mm)	SVA	153	105	137	118—148
	DMV	168	126	142	134—155
	NJ	165	149	157	152—162
	LI	163	153	157	154—161
	SNE	167	164	166	165—167
	GBK	149	144	147	145—149
Average Length (mm)	SVA	124	71	88	79—106
	DMV	127	103	114	108—120
	NJ	131	123	127	124—129
	LI	140	124	128	126—134
	SNE	146	115	141	128—144
	GBK	131	102	110	104—122

Specific Mortality Rate

The estimated constant specific mortality rate varied within and across survey regions (Table 3). The highest specific mortality rate of 0.58 yr^{-1} occurred in the Southern Virginia survey region in the 2000s (Table 3). This survey region also showed the largest range of specific mortality rates (Table 6, Fig. 7). Specific mortality rates from the survey regions in the central MAB were similar and showed little variability over the four decades (Table 3). In the Southern New England survey region, the constant specific mortality rates were the lowest, averaging 0.13 yr^{-1} over the four decades (Table 3). The constant specific mortality rate estimated for the Southern Virginia survey region showed the largest range (Table 3, Fig. 7A).

The average age-dependent specific mortality rates are higher in southern regions than the constant rates (Table 4). The largest average age-dependent mortality rate of 0.20 yr^{-1} was associated with the Georges Bank survey region. The specific age-dependent mortality rates estimated for the central MAB survey regions were the least variable, with maximum values that ranged between 0.17 and 0.20 yr^{-1} over the four decades (Table 4, Fig. 7B).

The overall averages for both specific constant and age-dependent mortality rates were similar (about 0.20 yr^{-1}). The age-dependent mortality rate regional median values were closer to the overall average than the constant mortality rate. Although, the variability of the constant mortality rate was driven mainly by values obtained for the Southern Virginia survey region, which was not included in the age-dependent mortality rate analysis.

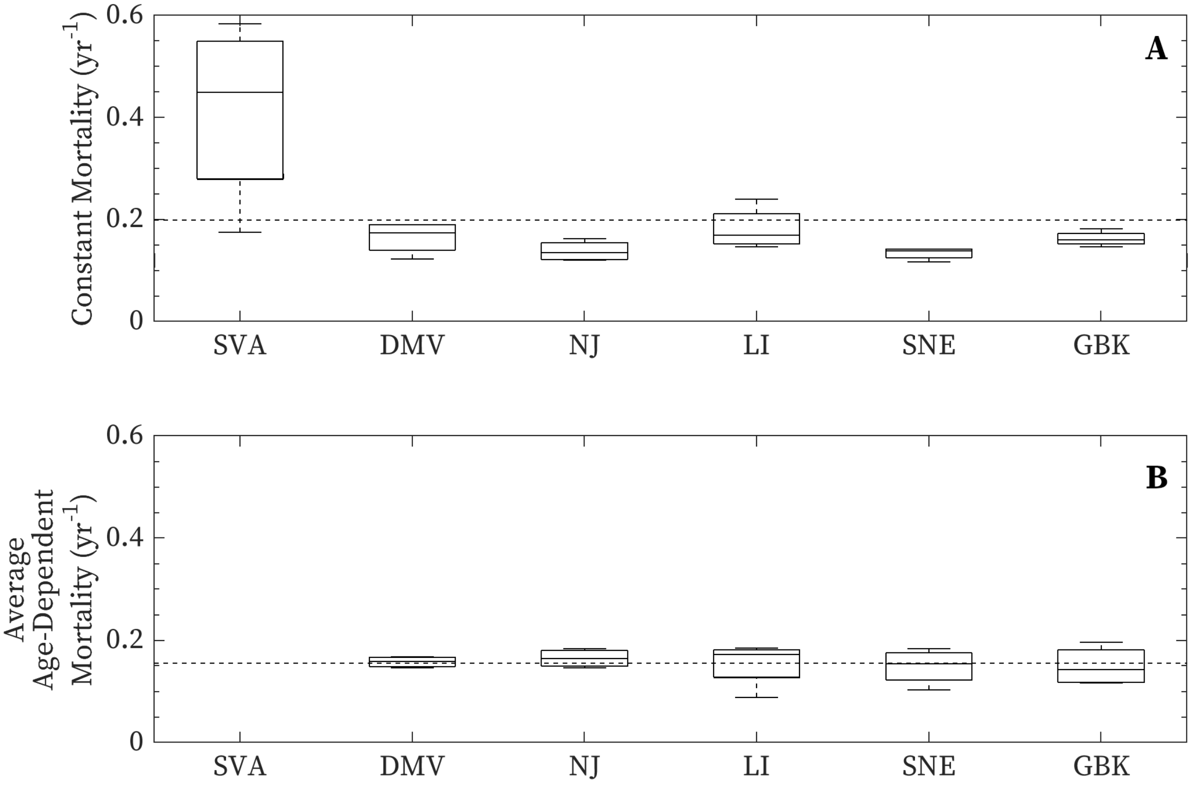

Figure 7. Range of Atlantic surfclam (A) constant specific mortality rate (yr^{-1}) calculated using Equation (3), and (B) age-dependent specific mortality rate (yr^{-1}) calculated using Equation (5). The decadal median (solid line), maximum and minimum (vertical lines) for each survey region, and the overall average for the MAB (dotted line) are shown. The age-dependent mortality was calculated for five of the six survey regions; Southern Virginia (SVA) was excluded from the calculation (see section *Mortality Rate* for details). The survey regions are ordered from south to north along the MAB (see Fig. 1) and defined as: Southern Virginia (SVA), Delmarva Peninsula (DMV), New Jersey (NJ), Long Island (LI), Southern New England (SNE), and Georges Bank (GBK).

TABLE 6.

Summary of the maximum, minimum, and median specific mortality rate (yr^{-1}) and age-dependent specific mortality rate (yr^{-1}) estimated from the Atlantic surfclam age and length observations for each survey region and each decade. The difference between the 0.25 and 0.75 quantiles indicates the variability of the data.

	Survey Region	Maximum	Minimum	Median	Quantiles (0.25 — 0.75)
Constant Mortality (yr^{-1})	SVA	0.58	0.18	0.45	0.28 — 0.22
	DMV	0.19	0.12	0.17	0.14—0.19
	NJ	0.16	0.12	0.14	0.12—0.16
	LI	0.24	0.15	0.17	0.15—0.21
	SNE	0.14	0.12	0.14	0.13—0.14
	GBK	0.18	0.15	0.16	0.15—0.17
Age-Dependent Mortality (yr^{-1})	SVA	–	–	–	—
	DMV	0.17	0.15	0.16	0.15—0.17
	NJ	0.18	0.15	0.16	0.15—0.18
	LI	0.19	0.09	0.17	0.13—0.18
	SNE	0.18	0.10	0.15	0.12—0.18
	GBK	0.20	0.12	0.14	0.12—0.18

Atlantic Surfclam Population Model

Effect of Specific Growth and Mortality Rates

The effect of specific growth and mortality rates on the Atlantic surfclam density was assessed by implementing the population dynamics model for a single representative ten-minute square, using the range of specific growth and mortality rates that encompass values estimated from age and length observations (Table 2, Table 3). The simulations were run for 100 years. The resulting simulations were then used to assess the relative importance of specific growth and mortality rates in controlling Atlantic surfclam population density. The density of the reproductive portion of the population and the density of recruits are indicators of the stability of the Atlantic surfclam population over time. The simulated reproductive density showed that the population specific mortality rate was more effective than the specific growth rate in controlling the number of Atlantic surfclams per meter square (Fig. 8B).

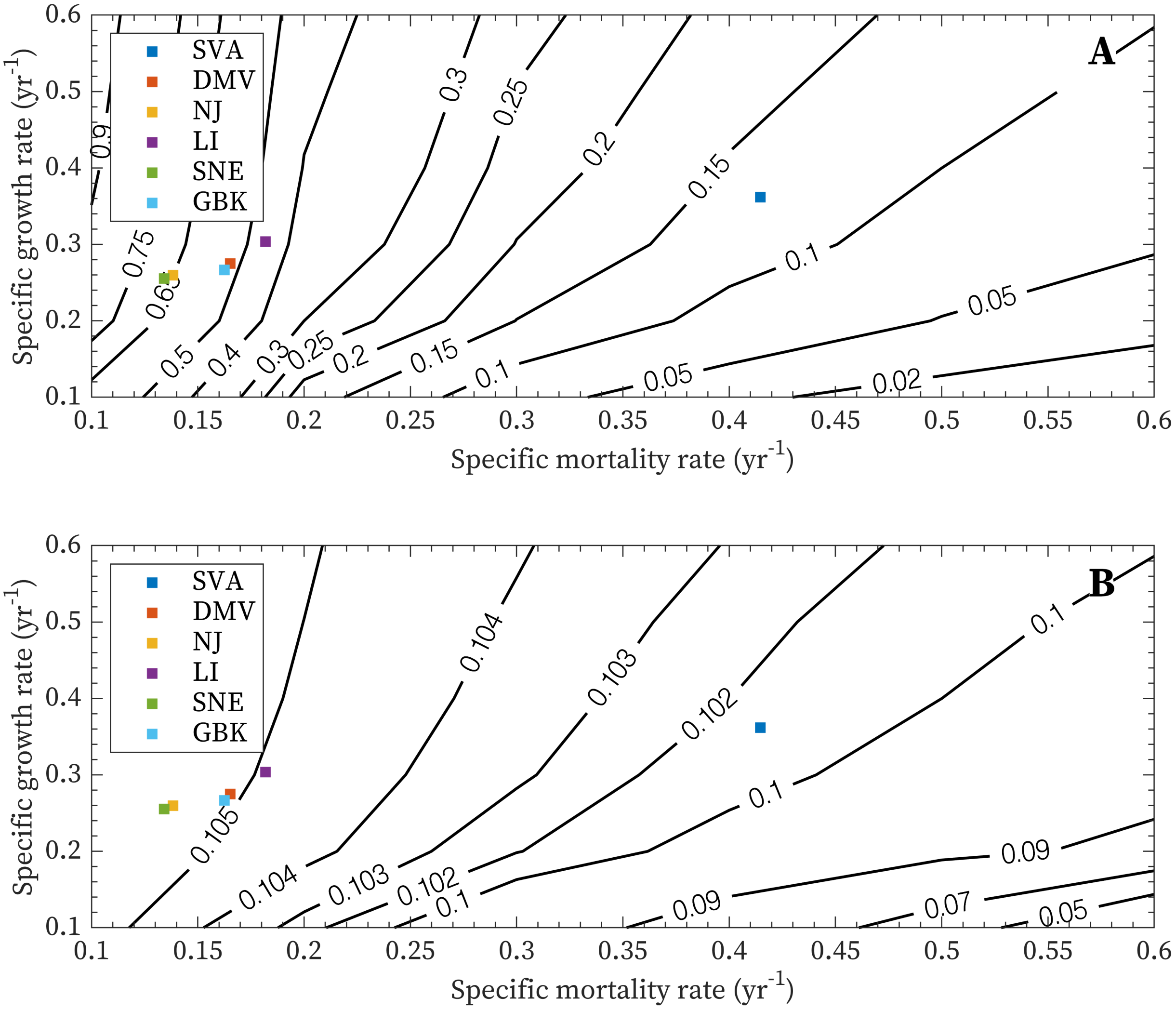

Figure 8. Simulated Atlantic surfclam (A) reproductive density (number m^{-2}) and (B) recruit density (number m^{-2}) for a range of constant specific mortality and growth rates. The average paired constant specific growth rate and specific mortality rate per survey region are shown (colors).

Simulation Characteristics

The specific growth and mortality rates estimated from the age and length observations (Table 3, Table 4) were input to the population model to simulate the time trajectory of the Atlantic surfclam population. Two sets of simulations that used a constant specific mortality rate (Equation 3) and an age-dependent mortality rate (Equation 5), respectively, were run for 100 years. The simulated Atlantic surfclam densities were averaged over the biological area included in the model to assess the effect of the different specific mortality rates for each decade.

The constant specific mortality rate resulted in an equilibrium density for the average Atlantic surfclam population of 1.2 Atlantic surfclam m^{-2} after 20 years (Fig. 9A). In contrast, the average Atlantic surfclam population using age-dependent mortality rates reached an equilibrium density of 0.9 Atlantic surfclams m^{-2} after 30 years (Fig. 9A). The average densities obtained for the 1990s and 2000s simulations did not show significant differences resulting from the different forms. Average densities during the 1990s were about 0.65 Atlantic surfclams m^{-2}, while during the 2000s, average densities were about 0.75 Atlantic surfclams m^{-2}. For both forms of specific mortality rate, the simulated Atlantic surfclam population begins to reproduce after one year (Fig. 9B, Fig. E.1B – E.2B), which maintains stable recruitment throughout the simulation. Small variations in recruitment resulted from the random process used to distribute recruits.

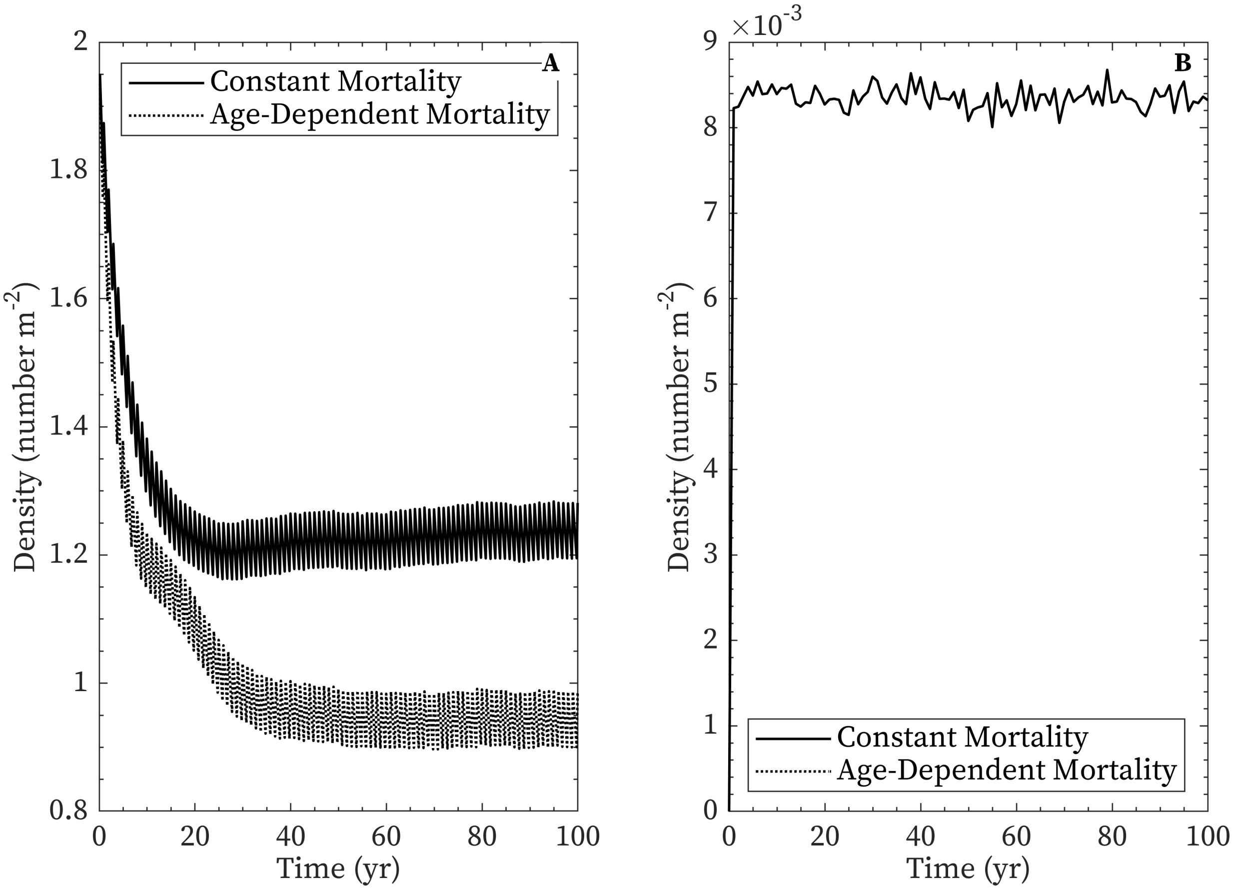

Figure 9. Simulated time evolution for Atlantic surfclam (A) reproductive clam density and (B) recruit density for the 2010s.

Effect of Mortality on Atlantic Surfclam Distribution

To assess the effect of mortality in controlling the Atlantic surfclam distribution, the population dynamics model was implemented using the specific growth rates and asymptotic lengths (Table 2), constant specific mortality rates (Table 3), and age-dependent specific mortality rates (Table 4) estimated for each survey region, and decade. Both mortality simulations were initialized with a constant Atlantic surfclam density of 2 m^{-2} over the entire model domain (Fig. 10A, Fig. 11A) and run for 100 years. The density distribution of the reproductive-sized Atlantic surfclams from the last year of the simulations was used for the analysis. The observed Atlantic surfclam density in each survey region for each decade provided a comparison for the simulated densities.

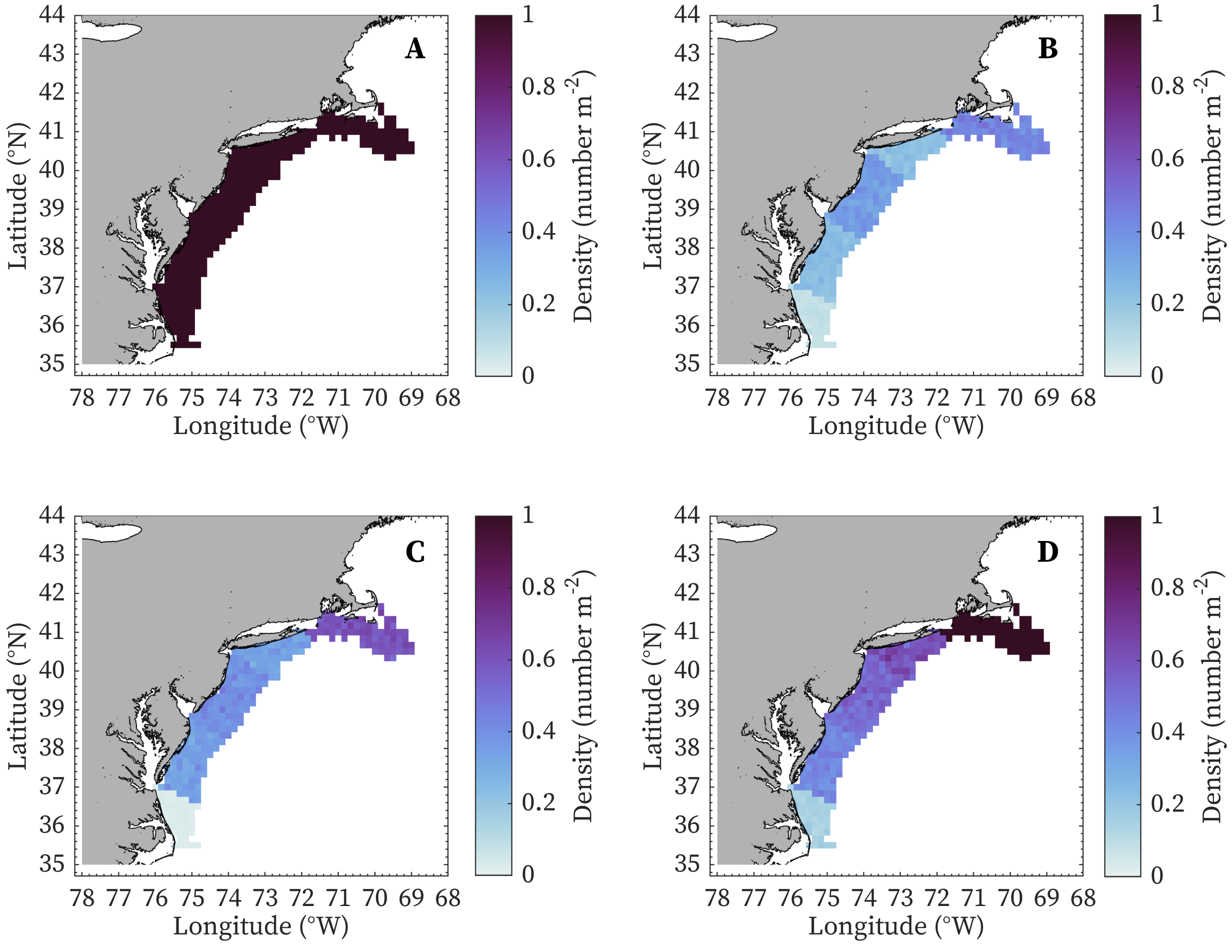

Figure 10. (A) Initial density distribution of reproductive-sized Atlantic surfclams used to obtain the simulated density distributions in each survey region for the (B) 1990s, (C) 2000s, and (D) 2010s. The simulations used the constant specific mortality rates (Table 3), specific growth rates, and asymptotic lengths (Table 2) estimated from the survey age and length observations.

A constant specific mortality rate produced heterogeneity in Atlantic surfclam density across the survey regions (Fig. 10). In the 1990s, simulated Atlantic surfclam density was high in the southern-most and northernmost survey regions, and densities of 0.5 to 0.7 Atlantic surfclam m^{-2} occurred in the other survey regions (Fig. 10B). In the 2000s, Atlantic surfclam densities increased in the northern survey regions and decreased to 0.1 to 0.4 Atlantic surfclams m^{-2} in the two southern survey regions (Fig. 10C). By 2010s, the simulated Atlantic surfclam density decreased in all but the northernmost survey region (Fig. 10D). Throughout the three decades, the northernmost region sustained high densities, >0.9 Atlantic surfclams m^{-2}, while regions in the middle (New Jersey and Long Island) remained above 0.7 Atlantic surfclam m^{-2}.

The simulated Atlantic surfclam density distribution produced using age-dependent specific mortality rates showed lower densities in the 1990s relative to the densities obtained with a constant specific mortality rate (Fig. 11B versus Fig. 10B). In the 2000s, simulated densities were highest in the central survey regions (Fig. 11C). The lowest densities, 0.3 to 0.4 Atlantic surfclams m^{-2}, were located in the southernmost and northernmost survey regions (Fig. 11C), in contrast to the densities obtained with a constant specific mortality rate (Fig. 10C). The simulated densities for the 2010s in the central survey regions remained constant in relation with the previous decade, while the highest (0.9 to 1.0 Atlantic surfclams m^{-2}) were located in the northernmost survey region (Fig. 11D); a density distribution much different from that obtained for the 2010s with a constant specific mortality rate (Fig. 10D).

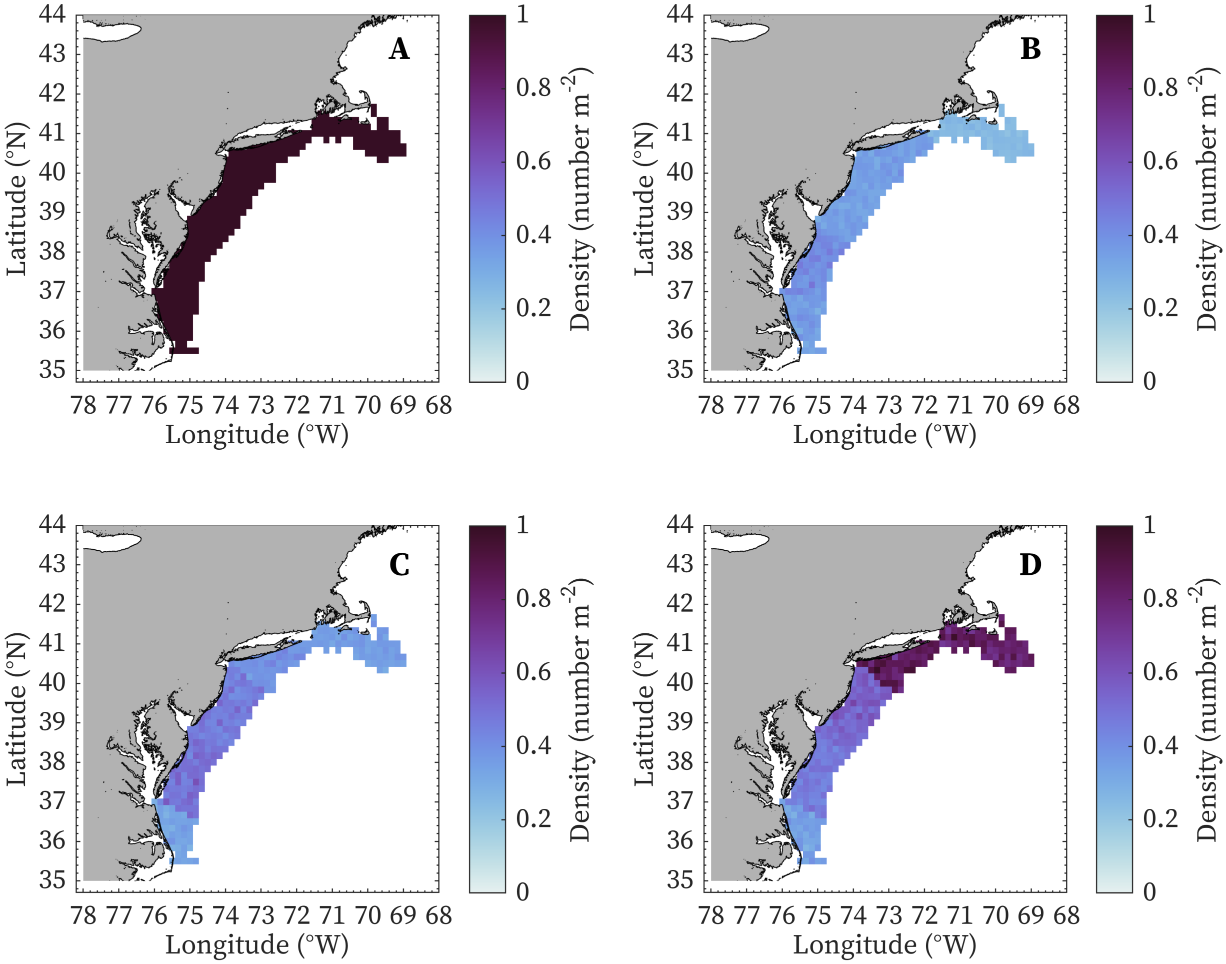

Figure 11. (A) Initial density distribution of reproductive-sized Atlantic surfclams used to obtain the simulated density distributions in each survey region for the (B) 1990s, (C) 2000s, and (D) 2010s. The simulations used the age-dependent specific mortality rates (Table 4), and specific growth rates and asymptotic lengths (Table 2) estimated from the survey age and length observations.

The RMSE between the observed and simulated densities in each survey region (Fig. 12) gives the relative effect of constant versus age-dependent specific mortality rates on Atlantic surfclam density distribution. The lowest and highest RMSEs for the constant specific mortality simulations were associated with the Southern Virginia and Southern New England survey regions, respectively

(Fig. 12A, Table 7). These survey regions also had the widest range in RMSE. The median values for the central survey regions ranged between 0.31 and 0.38 Atlantic surfclams m^{-2} (Table 7), with the RMSE associated with the Delmarva Peninsula region showing the smallest range (Fig. 12A). The RMSE associated with the simulated Atlantic surfclam densities from the age-dependent specific mortality rates simulations were overall smaller with a reduced range relative to those from the constant mortality simulations (Fig. 12B versus 12A).

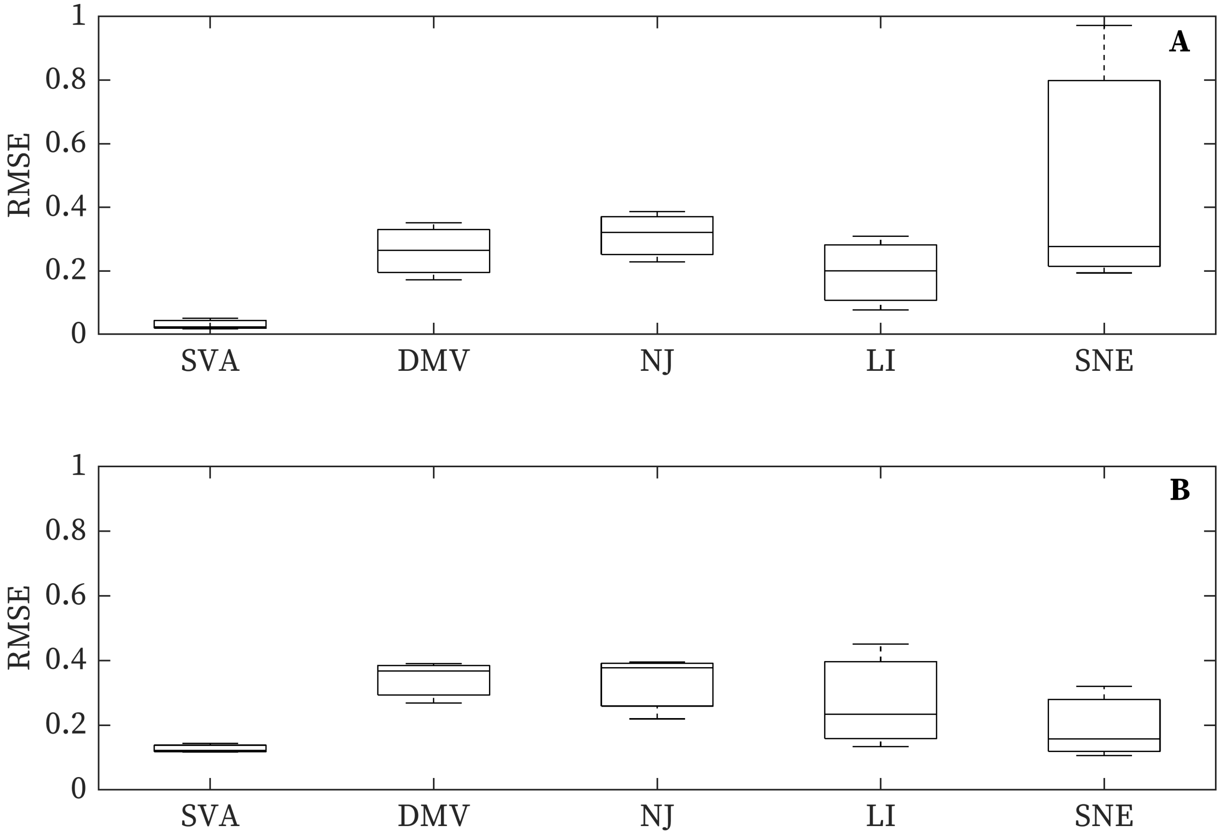

Figure 12. Root Mean Square Error (RMSE, Equation 11) for each survey region calculated using observed Atlantic surfclam densities and densities from simulations that used (A) constant specific mortality rates, and (B) age-dependent specific mortality rates. Survey regions are defined in Figure 1.

TABLE 7.
Summary of the maximum, minimum, and median Root Mean Square Error (RMSE) calculated for each survey region between observed Atlantic surfclam densities and densities obtained from simulations that used a constant specific mortality rate and age-dependent specific mortality rate. The difference between the 0.25 and 0.75 quantiles indicates the variability of the data. The survey regions are defined in Figure 1.

	Survey Region	Maximum	Minimum	Median	Quantiles (0.25 — 0.75)
RMSE Constant Specific Mortality Rate (number m^{-2})	SVA	0.05	0.02	0.02	0.02—0.04
	DMV	0.35	0.17	0.26	0.20—0.33
	NJ	0.39	0.23	0.32	0.25—0.37
	LI	0.31	0.07	0.20	0.11—0.28
	SNE	0.97	0.19	0.28	0.21—0.79
RMSE Age-Dependent Specific Mortality Rate (number m^{-2})	SVA	0.14	0.12	0.12	0.12—0.14
	DMV	0.39	0.26	0.37	0.29—0.42
	NJ	0.39	0.22	0.38	0.26—0.39
	LI	0.45	0.14	0.23	0.16—0.40
	SNE	0.32	0.10	0.16	0.12—0.29

The bias between the simulated and observed Atlantic surfclam densities was lowest in the Southern Virginia survey region for the constant and age-dependent specific mortality rates (Fig. 13A, B). Overall, the bias was largest for the constant specific mortality rate simulations in all survey regions (Fig. 13A, Table 8). The age-dependent specific mortality rate resulted in a reduction in the bias in all survey regions (Fig. 13B), with the largest reduction of about 40% associated with the New Jersey survey region (Table 8).

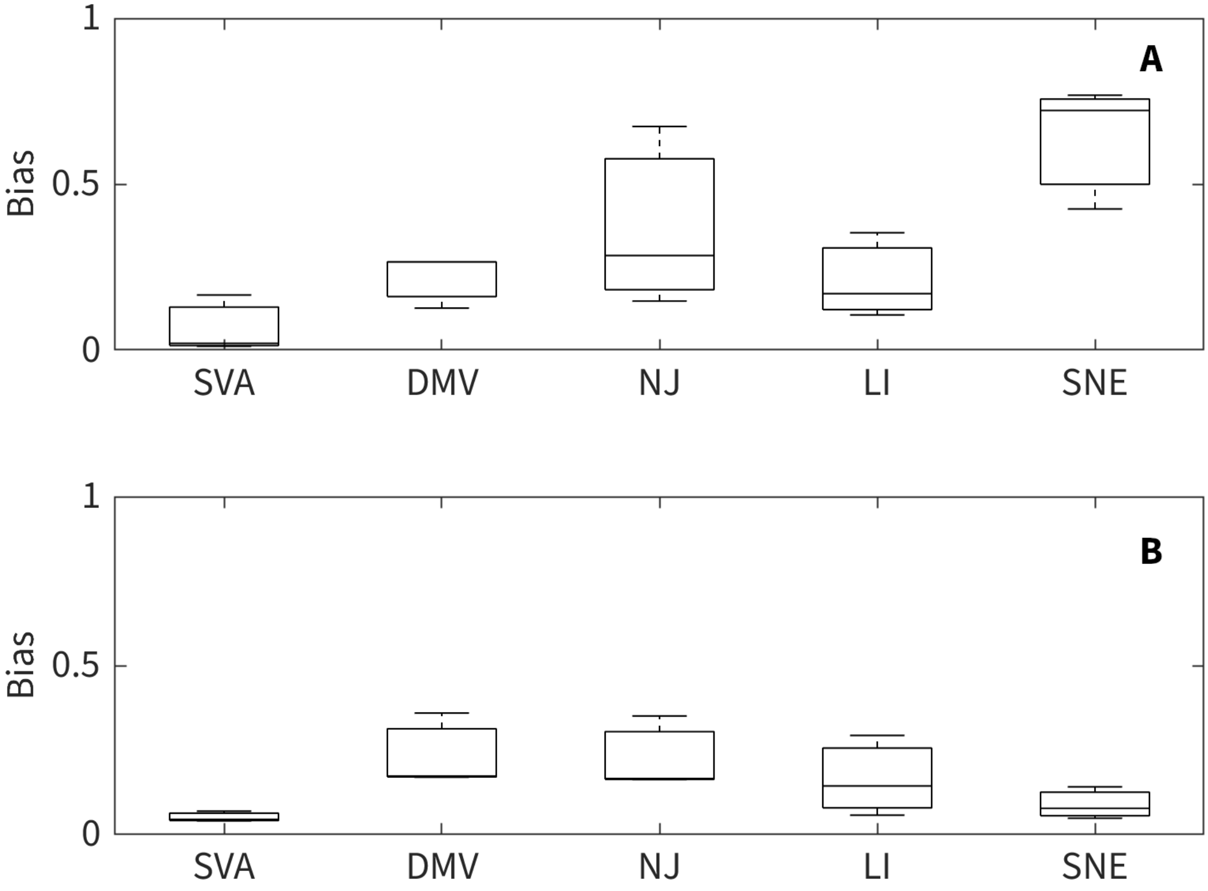

Figure 13. Bias, calculated using Equation (12), for each survey region between observed Atlantic surfclam densities and densities from simulations that used (A) constant specific mortality rates, and (B) age-dependent specific mortality rates. Survey regions are defined in Figure 1.

TABLE 8.
Summary of the maximum, minimum, and median Bias calculated for each survey region between observed Atlantic surfclam densities and densities obtained from simulations that used a constant specific mortality rate and age-dependent specific mortality rate. The difference between the 0.25 and 0.75 quantiles indicates the variability of the data. The survey regions are defined in Figure 1.

	Survey Region	Maximum	Minimum	Median	Quantiles (0.25 — 0.75)
Bias Constant Specific Mortality Rate (number m^{-2})	SVA	0.17	0.01	0.02	0.02—0.13
	DMV	0.27	0.13	0.27	0.16—0.27
	NJ	0.67	0.15	0.29	0.18—0.58
	LI	0.35	0.11	0.17	0.12—0.31
	SNE	0.77	0.43	0.72	0.50—0.76
Bias Age-Dependent Specific Mortality Rate (number m^{-2})	SVA	0.07	0.04	0.04	0.04—0.06
	DMV	0.36	0.17	0.17	0.17—0.31
	NJ	0.35	0.16	0.17	0.16—0.30
	LI	0.29	0.06	0.14	0.08—0.26
	SNE	0.14	0.05	0.08	0.06—0.13

The age-dependent specific mortality rate significantly reduced the precision ratio between the simulated and observed Atlantic surfclam densities (Fig. 14A, B). The reduction in the precision ratio was most pronounced for the New Jersey, Long Island, and Southern New England survey regions, with reductions of the median precision ratio of 40%, 35%, and 62%, respectively (Table 14). Although the magnitude was larger, the north-to-south trend in the precision ratio associated with the simulations that used a constant specific mortality rate was similar to that obtained from the age-dependent mortality rate simulations (Fig. 14).

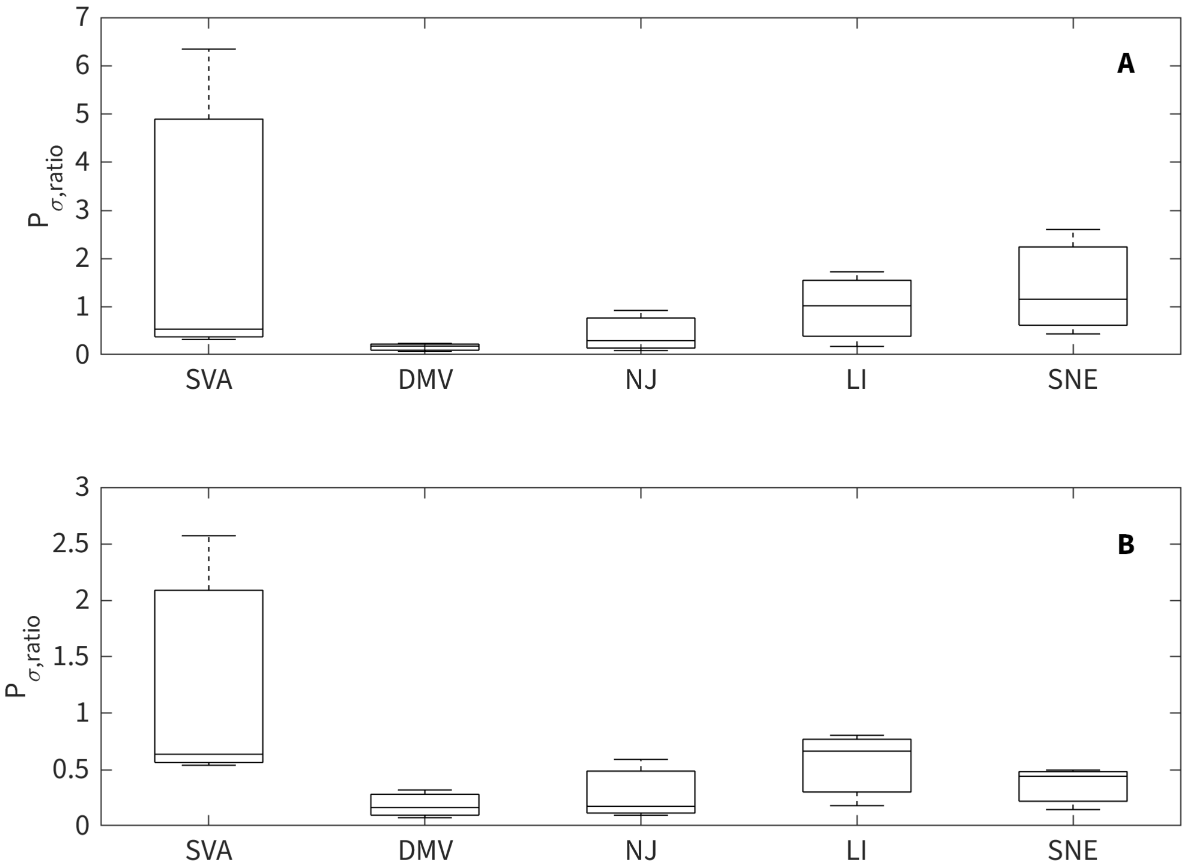

Figure 14. Precision ratio, $P_{\sigma,ratio}$, calculated using equation (13) for each survey region using the standard deviations of observed Atlantic surfclam densities and densities from simulations that used (A) constant specific mortality rates and (B) age-dependent specific mortality rates. Survey regions are defined in Figure 1.

TABLE 9.

Summary of the maximum, minimum, and median Precision, $P_{\sigma,ratio}$, calculated for each survey region between observed Atlantic surfclam densities and densities obtained from simulations that used a constant specific mortality rate and age-dependent specific mortality rate. The difference between the 0.25 and 0.75 quantiles indicates the variability of the data. The survey regions are defined in Figure 1.

	Survey Region	Maximum	Minimum	Median	Quantiles (0.25 — 0.75)
$P_{\sigma,ratio}$ Constant Specific Mortality Rate	SVA	6.34	0.33	0.54	0.38—4.89
	DMV	0.24	0.07	0.19	0.10—0.23
	NJ	0.93	0.10	0.30	0.15—0.77
	LI	1.73	0.18	1.02	0.39—1.55
	SNE	2.60	0.44	1.16	0.62—2.24
$P_{\sigma,ratio}$ Age-Dependent Specific Mortality Rate	SVA	2.57	0.54	0.64	0.56—2.08
	DMV	0.32	0.08	0.17	0.10—0.28
	NJ	0.59	0.10	0.18	0.12—0.49
	LI	0.80	0.18	0.66	0.30—0.77
	SNE	0.50	0.15	0.44	0.22—0.48

DISCUSSION

Population Growth Rate and Asymptotic Length

Weinberg & Helser (1996) applied a von Bertalanffy growth model to age and length data measured for Atlantic surfclam populations between Georges Bank and the Delmarva Peninsula in 1980 and from 1989 to 1992 to estimate specific growth rate and asymptotic length. Their analysis showed that the estimated specific growth rates and asymptotic length decreased off the Delmarva Peninsula and New Jersey between the two time periods. The parameter estimated for Long Island and Southern New England Atlantic surfclams showed no statistical difference. Weinberg & Helser (1996) attributed the decrease in growth parameters at the southern sites to an intense hypoxic event off New Jersey in the late 1970s and size-selective mortality imposed by commercial fishing. Subsequent studies (Weinberg 1998, 2005) confirmed that asymptotic lengths for Atlantic surfclam populations off the Delmarva Peninsula were smaller than in other areas of the MAB. The smaller length was attributed to density-dependent effects (Weinberg 1998) and poor condition due to warming bottom temperature (Weinberg 2005).

The asymptotic length estimates obtained in this study from the von Bertalanffy growth model using the age-length observations from the six survey regions showed a decreasing trend over the four decades for the Southern Virginia, Delmarva Peninsula, New Jersey, and Long Island survey regions.

The largest length decrease of 30% was associated with the Southern Virginia survey region. Asymptotic length showed no significant change in the Southern New England and Georges Bank survey region.

The previous analyses provided a progression of causes to explain changes in the growth characteristics of Atlantic surfclams, but none were definitive. The hypoxic event in the 1970s was a one-time extreme event and is unlikely to have a long-term effect across the range occupied by Atlantic surfclams. Atlantic surfclams have historically been lightly fished, and quota regulations have been set to maintain a stable catch (Hennen et al. 2018). The implication is that changes in Atlantic surfclam growth are the result of a forcing that is consistent and persistent over the range occupied by Atlantic surfclams.

Atlantic surfclams have a limited thermal tolerance, and since growth and maximum length are strongly dependent on temperature, bottom water temperatures that exceed the upper thermal range for Atlantic surfclams can result in physiological stress that reduces filtration and scope for growth, producing starvation and eventually mortality (Hornstein et al. 2018). Friedland et al. (2020) showed that water temperatures on the northeast U.S. continental shelf have warmed at an average rate of 0.24°C per decade from 1968 to 2018 and at 0.95°C per decade between 2004 and 2018. Warming of bottom waters was most pronounced in the fall at about 0.3°C per decade, with the most warming occurring in the southern portion of the northeast continental shelf. The change in the trend of asymptotic length, south-to-north, estimated for the survey regions for the 1980s to 2010s, is consistent with warming trends of MAB bottom temperatures that have occurred over the past four decades. The implication is that habitat alteration by warming bottom temperatures and subsequent reduction in the Cold Pool has affected the Atlantic surfclam population demographics over the MAB. This is consistent with the conclusion by Weinberg (2005) that the growth of Atlantic surfclam in the southern parts of the MAB was negatively impacted by warming bottom temperatures. Also, the empirical observations of poor conditions associated with Atlantic surfclams in the southern regions of the MAB, which was attributed to starvation (Marzec et al. 2010), are consistent with accumulated stress from exposure to warm temperatures (Munroe et al. 2013).

Historical estimates for MAB Atlantic surfclam specific growth rates range from 0.17 yr^{-1} to 0.25 yr^{-1} (Weinberg & Helser 1996, Weinberg 1999), with the smaller rates associated with southern MAB populations (Weinberg & Helser 1996). The specific growth rates estimated from the Southern Virginia stock surveys were the highest of all survey regions, with values that were more than double the estimates given by (Weinberg 1999). The high growth rates estimated for this survey region were associated with asymptotic lengths less than 150 mm. This combination of parameters is characteristic of small animals in the early phases of growth and is, therefore, not a good indicator of population viability because a significant fraction of the reproductive population is not present. The Delmarva Peninsula survey region also showed an increasing growth rate and decreasing asymptotic length over the four decades. The implication is that Atlantic surfclam populations in these regions are either in the early stages of being established or are in the latter stages of decline.

Munroe (2016) used an Atlantic surfclam growth model with a 50-years hindcast (1958-2007) of bottom water temperature on the MAB to investigate warming temperature versus commercial fishing effects on asymptotic length. This analysis showed a decrease in Atlantic surfclam asymptotic length of about 15 mm to 20 mm in the survey region off New Jersey and suggested that sustained bottom water temperatures that are 2°C warmer than average conditions can cause this decrease. The estimated asymptotic lengths for the New Jersey survey region show a decrease of about 15 mm over the four decades but with specific growth rates that are consistent with historical values. The implication is that the New Jersey Atlantic surfclam population is stable but may be in the early stages of decline.

Population Specific Mortality Rate

The first estimate of the natural specific mortality rate for Atlantic surfclams of 0.22 yr^{-1} was based on surveys made in the 1980s and 1990s for the population of the Delmarva Peninsula (Weinberg 2005). The decadal-average constant specific mortality rate estimated in this study of 0.2 yr^{-1} is similar to this rate. However, the individual constant specific mortality rates estimated for each decade for the Delmarva Peninsula region are lower by 13% to 45% relative to the value reported by Weinberg (2005). The age-dependent specific mortality rates estimated for the Delmarva Peninsula region were also lower.

The Atlantic surfclam population in the Delmarva Peninsula region was characterized by small asymptotic lengths, which resulted in the von Bertalanffy equation yielding high growth rates (a steeper slope to the growth curve). The high growth rate indicates the rate at which the small animals reach a maximum size. This is not an indicator of population viability since it only accounts for a fraction of the reproductive biomass. The survey region with high specific growth rates and small asymptotic length also had higher constant specific mortality rates.

The Hoenig (1983) relationship used to estimate the mortality rate is based on the oldest individual in the sample rather than the age distribution of the entire population. As a result, a shrinking population, one that is getting smaller, overestimates mortality. This may explain the higher mortality rate estimated by Weinberg (2005) because the Delmarva Peninsula population was declining in the late 1990s and early 2000s. Also, the correspondence between the decadal averaged constant mortality estimated from this study, and the Weinberg (2005) value may be because the decadal average included mostly shrinking populations in the southern survey regions.

The age-dependent specific mortality rate allows the age frequency distribution of the Atlantic surfclam population to influence the mortality rate. The age-length observations showed that the mortality rate is high at small sizes, levels out at intermediate ages, and increases at older ages. This pattern reflects the high predation mortality suffered by small post-settlement animals and the lessening of mortality rate as animals reach a size that allows escaping from predation mortality. Increased mortality at older aged Atlantic surfclams is likely from senescence, which has been observed in other bivalve species (e.g., Hofmann et al. 2006). The decadal averaged constant, and age-dependent specific mortality rates were similar. However, the distribution of mortality over the population is different, with the age-dependent mortality supporting higher survival of the older reproductive animals.

Atlantic Surfclam Density Distribution

Atlantic surfclams extend along the MAB continental shelf from intertidal regions to about 60 m (Jacobson & Weinberg 2006). Commercially viable densities of Atlantic surfclam occur off New York and New Jersey, southward to off the Delmarva Peninsula, along Southern New England, and north on Georges Bank (McCay et al. 2011). This general distribution is maintained by the dispersal of the Atlantic surfclam planktonic larvae and subsequent recruitment to the population (Zhang et al. 2015, 2016). However, Atlantic surfclam densities vary throughout the habitat (Timbs et al. 2019). This variability can arise from local processes that affect recruitment success (Weinberg 1999, Chintala & Grassle 2001) and/or conditions that affect the survival of the post-settlement population, such as food resources (Munroe et al. 2013) and bottom water temperature (Timbs et al. 2018).

This analysis showed that the form of local mortality pressure is an important factor controlling the observed gradient in Atlantic surfclam density along the MAB. The simulated spatial distribution densities obtained with a constant specific mortality rate not just overestimated densities in the survey regions relative to observed densities but also accentuated density heterogeneity along the MAB. Age-dependent specific mortality rates yielded simulated density gradients that closely matched observed densities, especially in the survey regions along the central portion of the MAB.

The age-dependent mortality rate reduced the discrepancy in simulated and observed densities in the Southern New England survey region by almost a factor of 10, smoothing out the heterogeneity in distribution. The exception was the Southern Virginia survey region, where the Atlantic surfclam age frequency distribution lacked sufficient representation of older animals to support the development of an age-based specific mortality rate.

The Atlantic surfclam populations in the central MAB and Southern New England survey regions are sufficiently stable to develop a robust age frequency distribution that supports an age-dependent mortality parameterization. The population structure in the Southern Virginia survey region was similar to that reported for Atlantic surfclams off New Jersey and the Delmarva Peninsula in the 1970s and 1980s (Weinberg 1999). For these populations, Weinberg (1999) estimated a mean specific adult mortality rate of 0.26 yr^{-1}, which included the effect of fishing. Fishing mortality for Atlantic surfclams is estimated as 0.12 yr^{-1} (Hennen et al. 2018), which makes the estimate by Weinberg (1999) similar to the decadal average constant specific mortality rate, 0.17 yr^{-1}, applied to the Southern Virginia survey region for the spatial simulations. The implication is that this specific mortality rate is representative of mortality rates for Atlantic surfclam populations with an age frequency dominated by early-age animals.

CONCLUSION

Warming ocean temperatures are known to generate important changes in local fisheries and ecosystems (Friedland & Hare 2007), resulting in range shifts in the distribution of many species (e.g., Beaugrand et al. 2002, Lucey & Nye 2010). Bottom water temperatures along the MAB continental shelf have warmed over the past few decades (Friedland et al. 2020, 2022), with effects on benthic species, especially those that depend on the Cold Pool.

Since the 1990s, decreases in the biomass of Atlantic surfclams have been observed at the southernmost locations of the species' range on the MAB continental shelf (NEFSC 2017, 2022). Warming bottom water temperatures and changing atmospheric and hydrographic conditions have been suggested as the cause for increased mortality (2 – 9%) that produced this biomass decrease (e.g., Weinberg et al. 2002, Weinberg 2005, Munroe et al. 2013, Narváez et al. 2015). The biomass decrease is most pronounced for Atlantic surfclam populations in the inner MAB shelf displacing the population center towards the outer shelf in southern locations (Weinberg 2005, Narváez et al. 2015, Timbs et al. 2019). Transport of Atlantic surfclam larvae to the southern MAB locations that could enhance biomass is limited because of increased surface and bottom temperatures, which limit the range of the reproductive population (O'Connor et al. 2007, Zhang et al. 2016). However, the lack of recovery of the southern MAB Atlantic surfclam populations may not result from an insufficient larval supply (Zhang et al. 2015) but rather from the trend towards smaller animals that have occurred over the past four decades.

The largest (older) individuals in a population are usually targeted by commercial fisheries (Hornstein et al. 2018). The southern MAB Atlantic surfclam populations have not been subjected to fishing pressure for at least a decade (Munroe et al. 2013, Munroe 2016) but have not recovered.

The reduction in length seen for these populations can be an important indicator of the longevity of the population (Ridgway et al. 2011). Changes in body size can change local responses to the effects of environmental variability, which in turn determines the tendency to become locally extinct (Smith et al. 1995, Chiba 1998, Hadly et al. 1998). The smaller size of the southern MAB Atlantic surfclams may predispose these populations to extinction as bottom temperatures warm. Thus, body size and life history need to be incorporated in predictions to responses to climate change, fishery pressure, and conservation attempts (Kaustuv et al. 2001).

Understanding the potential effects of climate change on the commercially important species that inhabit the continental shelf of the United States North Atlantic coast is even more important now that this region has been designated for offshore development of clean and economically viable energy. There are at least six approved leases for the installation of offshore wind energy arrays along the MAB continental shelf. The impact of the proposed wind energy arrays on the Atlantic surfclam fishery is of particular concern because some of the approved lease sites overlap with areas where the Atlantic surfclam fishery operates (NEFSC 2022) and, as a result, have the potential to cause negative economic impacts for the fishery (Scheld et al. 2022).

Most analyses of the impact of offshore wind energy development have focused on the effects on pelagic animals due to the difficulty of sampling close to the wind turbine structures (Lindeboom et al. 2011, Franco et al. 2015, Raoux et al. 2017). However, some studies have shown that the benthic communities in the near vicinity of the wind turbine structures show little change (Coates et al. 2016) and that limited access to wind farm areas can act as a protected area for some organisms (Inger et al. 2009, Lindeboom et al. 2011, Bergström et al. 2013, Ashley et al. 2014, Coates et al. 2016). However, a full understanding of the response of the entire ecosystem remains to be determined (Boehlert & Gill 2010).

Projections of responses to the combined stress imposed by climate change and offshore wind energy development provide an approach for assessing ecosystems' future states. The understanding and quantification of past and ongoing changes in Atlantic surfclam populations provided in this study form a basis for developing these types of projections.

LITERATURE CITED

Abbott, R. T. 1974. American seashells, 2nd edition. New York, NY: Van Nostrand Reinhold Co. 663 pp.

Acquafredda, M. P., D. M. Munroe, L. M. R. Calvo & M. De Luca. 2019. The effect of rearing temperature on the survival and growth of early juvenile Atlantic surfclams (*Spisula solidissima*). *Aquac. Rep.* 13:100176.

Alexander, R. R., R. J. Stanton & R. Dodd. 1993. Influence of sediment grain size on the burrowing of bivalves: Correlation with distribution and stratigraphic persistence of selected neogene clams. *Palaios* 8:289–303.

Andres, M., G. G. Gawarkiewicz & J. M. Toole. 2013. Interannual sea level variability in the western North Atlantic: Regional forcing and remote response. *Geophys. Res. Lett.* 40:5915–5919.

Ashley, M. C., S. C. Mangi & L. D. Rodwell. 2014. The potential of offshore windfarms to act as marine protected areas–A systematic review of current evidence. *Mar. Policy* 45:301–309.

Beardsley, R. C. 1981. On estuarine and continental-shelf circulation in the Middle Atlantic Bight. In: Warren, B. A. & C. Wunsch, editors. Evolution of physical oceanography: scientific surveys in honor of Henry Stommel. Cambridge, MA: The MIT Press. pp. 198–233.

Beardsley, R. C. & C. D. Winant. 1979. On the mean circulation in the Mid-Atlantic Bight. *J. Phys. Oceanogr.* 9:612–619.

Beaugrand, G., P. C. Reid, F. Ibanez, J. A. Lindley & M. Edwards. 2002. Reorganization of North Atlantic marine copepod biodiversity and climate. *Science* 296:1692–1694.

Bergström, L., F. Sundqvist & U. Bergström. 2013. Effects of an offshore wind farm on temporal and spatial patterns in the demersal fish community. *Mar. Ecol. Progr. Ser.* 485:199–210.

Beverton, R. J. H. & S. J. Holt. 1993. On the Dynamics of Exploited Fish Populations. New York, NY: Chapman & Hall. 538 pp.

Bigelow, H. B. 1933. Studies of the waters on the continental shelf, Cape Cod to Chesapeake Bay. I. The cycle of temperature. *Pap. Phys. Oceanogr. Meteor.* 2:135.

Boehlert, G. W. & A. B. Gill. 2010. Environmental and ecological effects of ocean renewable energy development: a current synthesis. *Oceanography* 23:68–81.

Brown, W., W. Boicourt, C. Flagg, A. Gangopadhyay, O. Schofield, S. Glenn & J. Kohut. 2012. Mapping the Mid-Atlantic Cold Pool evolution and variability with ocean gliders and numerical models. *2012 Oceans* 1–6.

Cargnelli, L. M., S. J. Griesbach, D. B. Packer & E. Weissberger. 1999. Essential fish habitat source document. Atlantic surfclam, *Spisula solidissima*, life history and habitat characteristics. NOAA Technical Memorandum NMFS-NE-142, 13 pp.

Chapman, D. C. & R. C. Beardsley. 1989. On the origin of shelf water in the Middle Atlantic Bight. *J. Phys. Oceanogr.* 19:384–391.

Chen, K., G. G. Gawarkiewicz, S. J. Lentz & J. M. Bane. 2014. Diagnosing the warming of the

Northeastern US Coastal Ocean in 2012: A linkage between the atmospheric jet stream variability and ocean response. *J. Geophys. Res. Oceans* 119:218–227.

Chen, Z., E. Curchitser, R. Chant & D. Kang. 2018. Seasonal variability of the cold pool over the Mid-Atlantic Bight continental shelf. *J. Geophys. Res. Oceans* 123:8203–8226.

Chiba, S. 1998. Synchronized evolution in lineages of land snails in oceanic islands. *Paleobiology* 24:99–108.

Chintala, M. M. & J. P. Grassle. 2001. Comparison of recruitment frequency and growth of surfclams, *Spisula solidissima* (Dillwyn, 1817), in different inner-shelf habitats of New Jersey. *J. Shellfish Res.* 20:1177–1186.

Coates, D. A., D. A. Kapasakali, M. Vincx & J. Vanaverbeke. 2016. Short-term effects of fishery exclusion in offshore wind farms on macrofaunal communities in the Belgian part of the North Sea. *Fish. Res.* 179:131–138.

Davis, C. W. 1979. Bottom-water temperature trends in the Middle Atlantic Bight during spring and autumn, 1964-76. NOAA Technical Memorandum NMFS SSRF-739, 17 pp.

DeFur, P. L. & C. P. Mangum. 1979. The effects of environmental variables on the heart rates of invertebrates. *Comp. Biochem. Physiol. A. Mol. Integr. Physiol.* 62:283–294.

Dillwyn, L. W. 1817. A Descriptive Catalogue of Recent Shells: Arranged According to the Linnæan Method; with Particular Attention to the Synonymy. London, UK: J. and A. Arch Cornhill. 1092 pp.

Ford, W. L., J. R. Longard & R. E. Banks. 1952. On the nature, occurrence and origin of cold low salinity water along the edge of the Gulf Stream. *J. Mar. Res.* 11:281-293.

Franco, A., V. Quintino & M. Elliott. 2015. Benthic monitoring and sampling design and effort to detect spatial changes: A case study using data from offshore wind farm sites. *Ecol. Indic.* 57:298–304.

Freitas, V., J. F. M. F. Cardoso, S. Santos, J. Campos, J. Drent, S. Saraiva, J. I. J. Witte, S. A. L. M. Kooijman & H. W. Van der Veer. 2009. Reconstruction of food conditions for Northeast Atlantic bivalve species based on Dynamic Energy Budgets. *J. Sea Res.* 62:75–82.

Friedland, K. D. & J. A. Hare. 2007. Long-term trends and regime shifts in sea surface temperature on the continental shelf of the Northeast United States. *Cont. Shelf. Res.* 27:2313–2328.

Friedland, K. D., R. E. Morse, J. P. Manning, D. C. Melrose, T. Miles, A. G. Goode, D. C. Brady, J. T. Kohut & E. N. Powell. 2020. Trends and change points in surface and bottom thermal environments of the US Northeast Continental Shelf Ecosystem. *Fish. Oceanogr.* 29:396–414.

Friedland, K. D., T. Miles, A. G. Goode, E. N. Powell & D. C. Brady. 2022. The Middle Atlantic Bight Cold Pool is warming and shrinking: Indices from in situ autumn seafloor temperatures. *Fish. Oceanogr.* 31:217–223.

Gangopadhyay, A., G. Gawarkiewicz, E. N. S. Silva, A. M. Silver, M. Monim & J. Clark. 2020. A census of the warm-core rings of the Gulf Stream: 1980–2017. *J. Geophys. Res. Oceans* 125:e2019JC016033.

Gangopadhyay, A., G. Gawarkiewicz, E. N. S. Silva, M. Monim & J. Clark. 2019. An observed regime shift in the formation of warm core rings from the Gulf Stream. *Sci. Rep.* 9:1–9.

Gawarkiewicz, G. G., R. E. Todd, A. J. Plueddemann, M. Andres & J. P. Manning. 2012. Direct interaction between the Gulf Stream and the shelfbreak south of New England. *Sci. Rep.* 2:1–6.

Hadly, E. A., M. H. Kohn, J. A. Leonard & R. K. Wayne. 1998. A genetic record of population isolation in pocket gophers during Holocene climatic change. *PNAS* 95:6893–6896.

Haggett, C., T. ten Brink, A. Russell, M. Roach, J. Firestone, T. Dalton & B. J. McCay. 2020. Offshore wind projects and fisheries. *Oceanography* 33:38–47.

Hennen, D. R., R. Mann, D. M. Munroe & E. N. Powell. 2018. Biological reference points for Atlantic surfclam (*Spisula solidissima*) in warming seas. *Fish. Res.* 207:126–139.

Hewitt, D. A. & J. M. Hoenig. 2005. Comparison of two approaches for estimating natural mortality based on longevity. *Fish. Bull.* 103:433–437.

Hoenig, J. M. 1983. Empirical use of longevity data to estimate mortality rates. *Fish. Bull.* 82:898–903.

Hofmann, E. E., J. M. Klinck, J. N. Kraeuter, E. N. Powell, R. E. Grizzle, S. C. Buckner & V. M. Bricelj. 2006. A population dynamics model of the hard clam, *Mercenaria mercenaria*: Development of the age-and length-frequency structure of the population. *J. Shellfish Res.* 25:417-444.

Hornstein, J., E. P. Espinosa, R. M. Cerrato, K. M. Lwiza & B. Allam. 2018. The influence of temperature stress on the physiology of the Atlantic surfclam, *Spisula solidissima*. *Comp. Biochem. Physiol. Part A Mol. Integr. Physiol.* 222:66–73.

Houghton, R. W., C. N. Flagg & L. J. Pietrafesa. 1994. Shelf-slope water frontal structure, motion and eddy heat flux in the southern Middle Atlantic Bight. *Deep Sea Res. Part II Top. Stud. Oceanogr.* 41:273–306.

Houghton, R. W., R. Schlitz, R. C. Beardsley, B. Butman & J. L. Chamberlin. 1982. The Middle Atlantic Bight cold pool: Evolution of the temperature structure during summer 1979. *J. Phys. Oceanogr.* 12:1019–1029.

Inger, R., M. J. Attrill, S. Bearhop, A. C. Broderick, W. James Grecian, D. J. Hodgson, C. Mills, E. Sheehan, S. C. Votier, M. J. Witt & B. J. Godley. 2009. Marine renewable energy: Potential benefits to biodiversity? An urgent call for research. *J. Appl. Ecol.* 46:1145–1153.

Jacobson, L. & J. Weinberg. 2006. Atlantic surfclam (*Spisula solidissima).* In: Status of Fishery Resources of the Northeastern US. NOAA/NEFSC Resource Evaluation and Assessment Division. 8 pp. Revised December 2006. Available at: http://www.nefsc.noaa.gov/sos/spsyn/iv/surfclam/index.html.

Jossi, J. W. & R. L. Benway. 2003. Variability of temperature and salinity in the Middle Atlantic Bight and Gulf of Maine based on data collected as part of the MARMAP Ships of Opportunity Program, 1978-2001. NOAA Technical Memorandum NMFS-NE-172. pp. 102.

Kang, D. & E. N. Curchitser. 2013. Gulf Stream eddy characteristics in a high-resolution ocean model. *J. Geophys. Res. Oceans* 118:4474–4487.

Kaustuv, R., D. Jablonski & J. W. Valentine. 2001. Climate change, species range limits and body size in marine bivalves. *Ecol. Lett.* 4:366-370.

Ketchum, B. H. 1964. The persistence of winter water on the continental shelf south of Long Island, New York. *Limnol. Oceanogr.* 9:467–475.

Kim, Y. & E. N. Powell. 2004. Surfclam histopathology survey along the Delmarva mortality line. *J. Shellfish Res.* 23:429–442.

Lentz, S. J. 2008. Seasonal variations in the circulation over the Middle Atlantic Bight continental shelf. *J. Phys. Oceanogr.* 38:1486–1500.

Lentz, S. J. 2017. Seasonal warming of the Middle Atlantic Bight Cold Pool. *J. Geophys. Res. Oceans* 122:941–954.

Levin, J., J. Wilkin, N. Fleming & J. Zavala-Garay. 2018. Mean circulation of the Mid-Atlantic Bight from a climatological data assimilative model. *Ocean Model.* 128:1–14.

Lindeboom, H. J., H. J. Kouwenhoven, M. J. N. Bergman, S. Bouma, S. Brasseur, R. Daan, R. C. Fijn, D. De Haan, S. Dirksen, R. Van Hal, R. Hille Ris Lambers, R. ter Hofstede, K. L. Krijgsveld, M. Leopold & M. Scheidat. 2011. Short-term ecological effects of an offshore wind farm in the Dutch coastal zone; a compilation. *Environ. Res. Lett.* 6:035101.

Linder, C. A. & G. G. Gawarkiewicz. 1998. A climatology of the shelfbreak front in the Middle Atlantic Bight. *J. Geophys. Res. Oceans* 103:18405–18423.

Link, J. S., A. Bundy, W. J. Overholtz, N. Shackell, J. Manderson, D. Duplisea, J. Hare, M. Koen-Alonso & K. D. Friedland. 2011. Ecosystem-based fisheries management in the Northwest Atlantic. *Fish Fish.* 12:152–170.

Loesch, J. G. & J. W. Ropes. 1977. Assessment of surf clam stocks in nearshore waters along the Delmarva Peninsula and in the fishery south of Cape Henry. *Proc. Natl. Shellfisheries Ass.* 67:29–34.

Loosanoff, V. L. & H. C. Davis. 1963. Rearing of bivalve mollusks. *Adv. Mar. Biol.* 1:1–136.

Lucey, S. M. & J. A. Nye. 2010. Shifting species assemblages in the Northeast US continental shelf large marine ecosystem. *Mar. Ecol. Progr. Ser.* 415:23-33.

Marzec, R. J., Y. Kim & E. N. Powell. 2010. Geographical trends in weight and condition index of surfclams (*Spisula solidissima*) in the Mid-Atlantic Bight. *J. Shellfish Res.* 29:117–128.

McCay, B. J., S. Brandt & C. F. Creed. 2011. Human dimensions of climate change and fisheries in a coupled system: the Atlantic surfclam case. *ICES J. Mar. Sci.* 68:1354–1367.

Methratta, E. T. 2020. Monitoring fisheries resources at offshore wind farms: BACI vs. BAG designs. *ICES J. Mar. Sci.* 77:890-900.

Mountain, D. G. 1991. The volume of shelf water in the Middle Atlantic Bight: Seasonal and interannual variability, 1977–1987. *Cont. Shelf Res.* 11:251–267.

Mountain, D. G. 2003. Variability in the properties of Shelf Water in the Middle Atlantic Bight, 1977–1999. *J. Geophys. Res. Oceans* 108:3014.

Munroe, D. M. 2016. Habitat effects on early post-settlement growth of intertidal clams, *Venerupis philippinarum* (A. Adams & Reeve, 1850). *J. Molluscan Stud.* 82:507–514.

Munroe, D. M., D. A. Narváez, D. Hennen, L. Jacobson, R. Mann, E. E. Hofmann, E. N. Powell & J. M. Klinck. 2016. Fishing and bottom water temperature as drivers of change in maximum shell length in Atlantic surfclams (*Spisula solidissima*). *Estuar. Coast. Shelf Sci.* 170:112–122.

Munroe, D. M., E. N. Powell, J. M. Klinck, A. M. Scheld, S. Borsetti, J. Beckensteiner & E. E.

Hofmann. 2022. The Atlantic surfclam fishery and offshore wind energy development: 1. Model development and verification. *ICES J. Mar. Sci.* 79:1787–1800.

Munroe, D. M., E. N. Powell, R. Mann, J. M. Klinck & E. E. Hofmann. 2013. Underestimation of primary productivity on continental shelves: evidence from maximum size of extant surfclam (*Spisula solidissima*) populations. *Fish. Oceanogr.* 22:220–233.

Myers, R. A., K. G. Bowen & N. J. Barrowman. 1999. Maximum reproductive rate of fish at low population sizes. *Can. J. Fish. Aquat. Sci.* 56:2404–2419.

Narváez, D. A., D. M. Munroe, E. E. Hofmann, J. M. Klinck, E. N. Powell, R. Mann & E. Curchitser. 2015. Long-term dynamics in Atlantic surfclam (*Spisula solidissima*) populations: the role of bottom water temperature. *J. Mar. Syst.* 141:136–148.

NEFSC. 1995. Report of the 19th Northeast Regional Stock Assessment Workshop (19th SAW). US Dept. Commer., Northeast Fish. Sci. Cent. Ref. Doc. 95-09. pp. 120–176.

NEFSC. 2017. 61st Northeast Regional Stock Assessment Workshop (61st SAW) Assessment Report. US Dept. Commer, Northeast Fish. Sci. Cent. Ref. Doc. 17-05. pp. 1–466.

NEFSC. 2022. Management Track Assessments Completed in Spring 2020. (22-09), 86. US Dept. Commer., Northeast Fish. Sci. Cent. Ref. Doc. 22-09, 86 pp.

O'Beirn, F. X., R. L. Walker, D. H. Hurley & D. A. Moroney. 1997. Culture of surfclams *Spisula solidissima sp.* in Coastal Georgia: nursery culture. *J. Shellfish Res.* 16:157–160.

O'Connor, M. I., J. F. Bruno, B. S. Gaines, Steven D andf Halpern, S. E. Lester, B. P. Kinlan

& J. M. Weiss. 2007. Temperature control of larval dispersal and the implications for marine ecology, evolution, and conservation. *PNAS* 104:1266–1271.

O'Leary, B. C., J. C. R. Smart, F. C. Neale, J. P. Hawkins, S. Newman, A. C. Milman & C. M. Roberts. 2011. Fisheries mismanagement. *Mar. Pollut. Bull.* 62:2642–2648.

O'Reilly, J. E. & D. A. Busch. 1984. Phytoplankton primary production on the northwestern Atlantic shelf. *Rapp. PV Reun. Cons. Int. Explor. Mer.* 183:255–268.

Powell, E. M. & R. J. Stanton. 1985. Estimating biomas and energy flow of molluscs in palaeocommunities. *Palaeontology* 28:1–34.

Powell, E. N., A. M. Ewing & K. M. Kuykendall. 2020. Ocean quahogs (*Arctica islandica*) and Atlantic surfclams (*Spisula solidissima*) on the Mid-Atlantic Bight continental shelf and Georges Bank: the death assemblage as a recorder of climate change and the reorganization of the continental shelf benthos. *Palaeogeogr. Palaeoclimatol. Palaeoecol.* 537:109205.

Powell, E. N., E. E. Hofmann, J. M. Klinck & S. M. Ray. 1992. Modeling oyster populations: I. A commentary on filtration rate. Is faster always better?. *J. Shellfish. Res.* 11:387–398.

Powell, E. N., R. Mann, K. A. Ashton-Alcox, Y. Kim & D. Bushek. 2016. The allometry of oysters: spatial and temporal variation in the length–biomass relationships for *Crassostrea virginica*. *J. Mar. Biol. Assoc. U. K.* 96:1127-1144.

Quijon, P. A., J. P. Grassle & J. M. Rosario. 2007. Naticid snail predation on early post-settlement surfclams (*Spisula solidissima*) on the inner continental shelf of New Jersey, USA. *Mar. Biol.* 150:873–882.

Raoux, A., S. Tecchio, J.-P. Pezy, G. Lassalle, S. Degraer, D. Wilhelmsson, M. Cachera, B. Ernande, C. Le Guen, M. Haraldsson, K. Grangeré, F. Le Loc'h, J. Dauvin & N. Niquil. 2017. Benthic and fish aggregation inside an offshore wind farm: Which effects on the trophic web functioning?. *Ecol. Indic.* 72:33–46.

Ridgway, I. D., C. A. Richardson & S. N. Austad. 2011. Maximum shell size, growth rate, and maturation age correlate with longevity in bivalve molluscs. *J. Gerontol. Biol. Sci. Med. Sci.* 66:183–190.

Ropes, J. W. 1968. Reproductive cycle of the surf clam, *Spisula solidissima*, in offshore New Jersey. *Biol. Bull.* 135:349–365.

Ropes, J. W. 1978. Biology and distribution of Surf Clams (*Spisula solidissima*) and Ocean Quahogs (*Arctica islandica*) Off the Northeast Coast of the United States. In: Proc. Northeast Clam Ind.: Management for the future. Univ. Mass. and Mass. Inst. Tech. Sea Grant Prog. SP-112, pp. 47 – 66.

Savage, N. B. 1976. Burrowing activity in *Mercenaria mercenaria* (L.) and *Spisula solidissima* (Dillwyn) as a function of temperature and dissolved oxygen. *Mar. Behav. Physiol.* 3:221–234.

Scheld, A. M., J. Beckensteiner, D. M. Munroe, E. N. Powell, S. Borsetti, E. E. Hofmann & J. M. Klinck. 2022. The Atlantic surfclam fishery and offshore wind energy development: 2. assessing economic impacts. *ICES J. Mar. Sci.* 79:1801–1814.

Seber, G. A. F. & C. J. Wild.. 2003. Nonlinear Regression. Hoboken. New Jersey: John Wiley & Sons. pp. 62–63.

Shearman, R. K. & S. J. Lentz. 2010. Long-term sea surface temperature variability along the US East Coast. *J. Phys. Oceanogr.* 40:1004–1017.

Smith, F. A., J. L. Betancourt & J. H. Brown. 1995. Evolution of body size in the woodrat over the past 25,000 years of climate change. *Science* 270:2012–2014.

Smolarkiewicz, P. K. & L. G. Margolin. 1998. MPDATA: A finite-difference solver for geophysical flows. *J. Comput. Phys.* 140:459–480.

Snelgrove, P. V. R., J. P. Grassle & C. A. Butman. 1998. Sediment choice by settling larvae of the bivalve, *Spisula solidissima* (Dillwyn), in flow and still water. *J. Exp. Mar. Biol. Ecol.* 231:171–190.

Timbs, J. R., E. N. Powell & R. Mann. 2018. Assessment of the relationship of stock and recruitment in the Atlantic surfclam *Spisula solidissima* in the northwestern Atlantic Ocean. *J. Shellfish Res.* 37:965–978.

Timbs, J. R., E. N. Powell & R. Mann. 2019. Changes in the spatial distribution and anatomy of a range shift for the Atlantic surfclam *Spisula solidissima* in the Mid-Atlantic Bight and on Georges Bank. *Mar. Ecol. Prog. Ser.* 620:77–97.

van der Meer, J. 2006. An introduction to Dynamic Energy Budget (DEB) models with special emphasis on parameter estimation. *J. Sea Res.* 56:85–102.

von Bertalanffy, L. 1938. A quantitative theory of organic growth (inquiries on growth laws. II). *Hum. biol.* 10:181–213.

Wallace, E. J., L. B. Looney & D. Gong. 2018. Multi-decadal trends and variability in temperature and salinity in the Mid-Atlantic Bight, Georges Bank, and Gulf of Maine. *J. Mar. Res.* 76:163–215.

Weinberg, J. R. 1993. Surfclam populations of the middle Atlantic, southern New England, and Georges Bank for 1992. Northeast Fish. Sci. Cent. Ref. Doc. 93-01. 27 pp.

Weinberg, J. R. 1998. Density-dependent growth in the Atlantic surfclam, *Spisula solidissima*, off the coast of the Delmarva Peninsula, USA. *Mar. Biol.* 130:621–630.

Weinberg, J. R. 1999. Age-structure, recruitment, and adult mortality in populations of the Atlantic surfclam, *Spisula solidissima*, from 1978 to 1997. *Mar. Biol.* 134:113–125.

Weinberg, J. R. 2005. Bathymetric shift in the distribution of Atlantic surfclams: response to warmer ocean temperature. *ICES J. Mar. Sci.* 62:1444–1453.

Weinberg, J. R. & T. E. Helser. 1996. Growth of the Atlantic surfclam, *Spisula solidissima*, from Georges Bank to the Delmarva Peninsula, USA. *Mar. Biol.* 126:663–674.

Weinberg, J. R., T. G. Dahlgren & K. M. Halanych. 2002. Influence of rising sea temperature on commercial bivalve species of the US Atlantic coast. *Am. Fish. Soc. Symp.* 32:131–140.

Xu, Y., R. Chant, D. Gong, R. Castelao, S. Glenn & O. Schofield. 2011. Seasonal variability of chlorophyll a in the Mid-Atlantic Bight. *Cont. Shelf Res.* 31:1640–1650.

Xu, Y., T. Miles & O. Schofield. 2020. Physical processes controlling chlorophyll-a variability on the Mid-Atlantic Bight along Northeast United States. *J. Mar. Syst.* 212:103433.

Yoder, J. A., S. E. Schollaert & J. E. O’Reilly. 2002. Climatological phytoplankton chlorophyll and sea surface temperature patterns in continental shelf and slope waters off the northeast US coast. *Limnol. Oceanogr.* 47:672–682.

Zhang, W. G. & G. G. Gawarkiewicz. 2015. Dynamics of the direct intrusion of Gulf Stream ring water onto the Mid-Atlantic Bight shelf. *Geophys. Res. Lett.* 42:7687–7695.

Zhang, X., D. Haidvogel, D. M. Munroe, E. N. Powell, J. Klinck, R. Mann & F. S. Castruccio. 2015. Modeling larval connectivity of the Atlantic surfclams within the Middle Atlantic Bight: Model development, larval dispersal and metapopulation connectivity. *Estuar. Coast. Shelf Sci.* 153:38–53.

Zhang, X., D. M. Munroe, D. Haidvogel & E. N. Powell. 2016. Atlantic surfclam connectivity within the Middle Atlantic Bight: mechanisms underlying variation in larval transport and settlement. *Estuar. Coast. Shelf. Sci.* 173:65–78.

APPENDICES

VON BERTALANFFY FIGURES

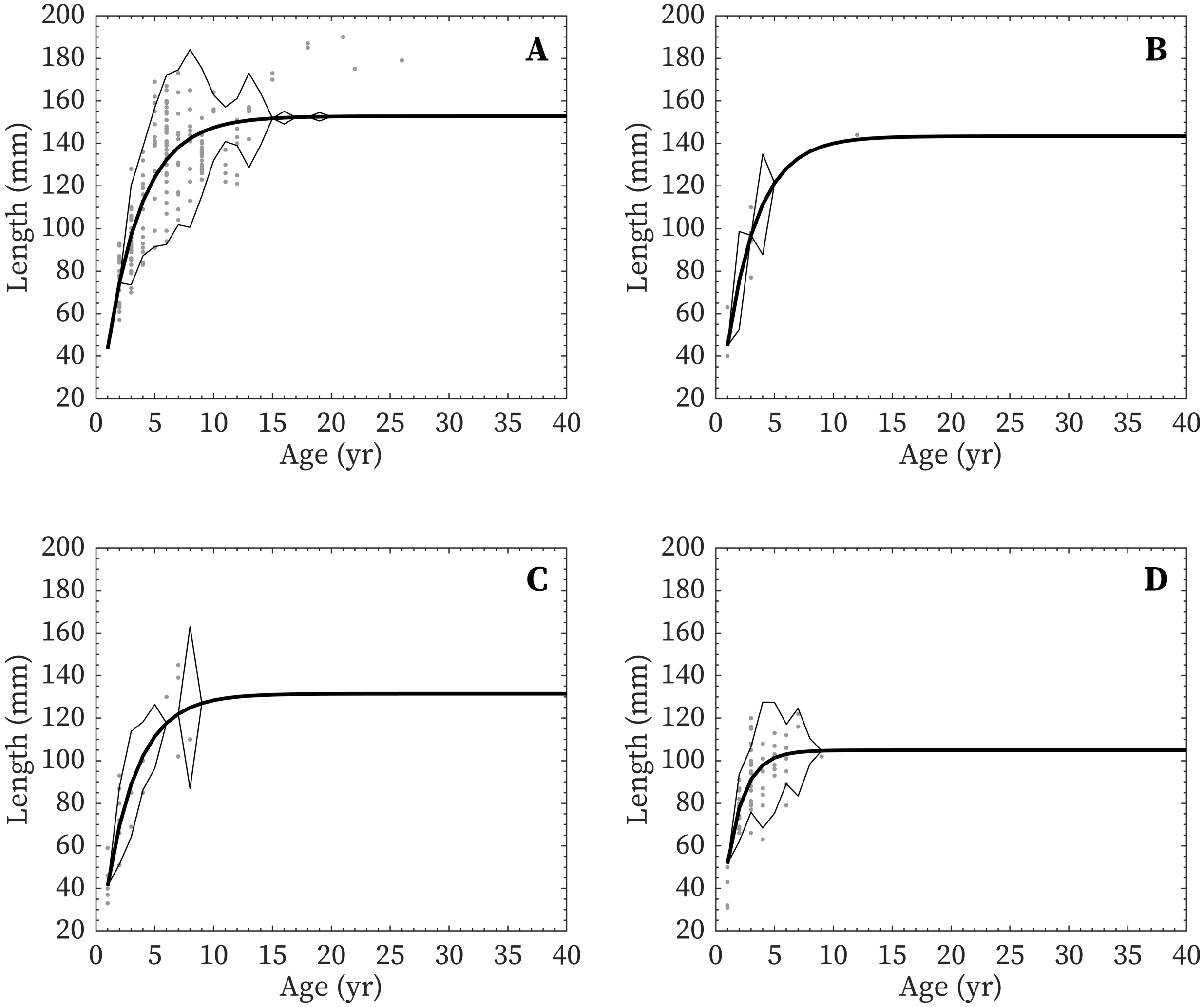

Figure A.1. Atlantic surfclam age (yr) versus length (mm) observations (grey dots) obtained from the Southern Virginia survey region for (A) 1980s, (B) 1990s, (C) 2000s, and (D) 2010s. The growth curve (heavy line) and standard deviation (2σ, thin line) obtained from the von Bertalanffy equation fit to the observations for each decade is shown. All curve fits are significant ($p < 0.001$) with r^2 values of 0.66 for the 1980s, 0.84 for the 1990s, 0.84 for the 2000s and 0.56 for the 2010s.

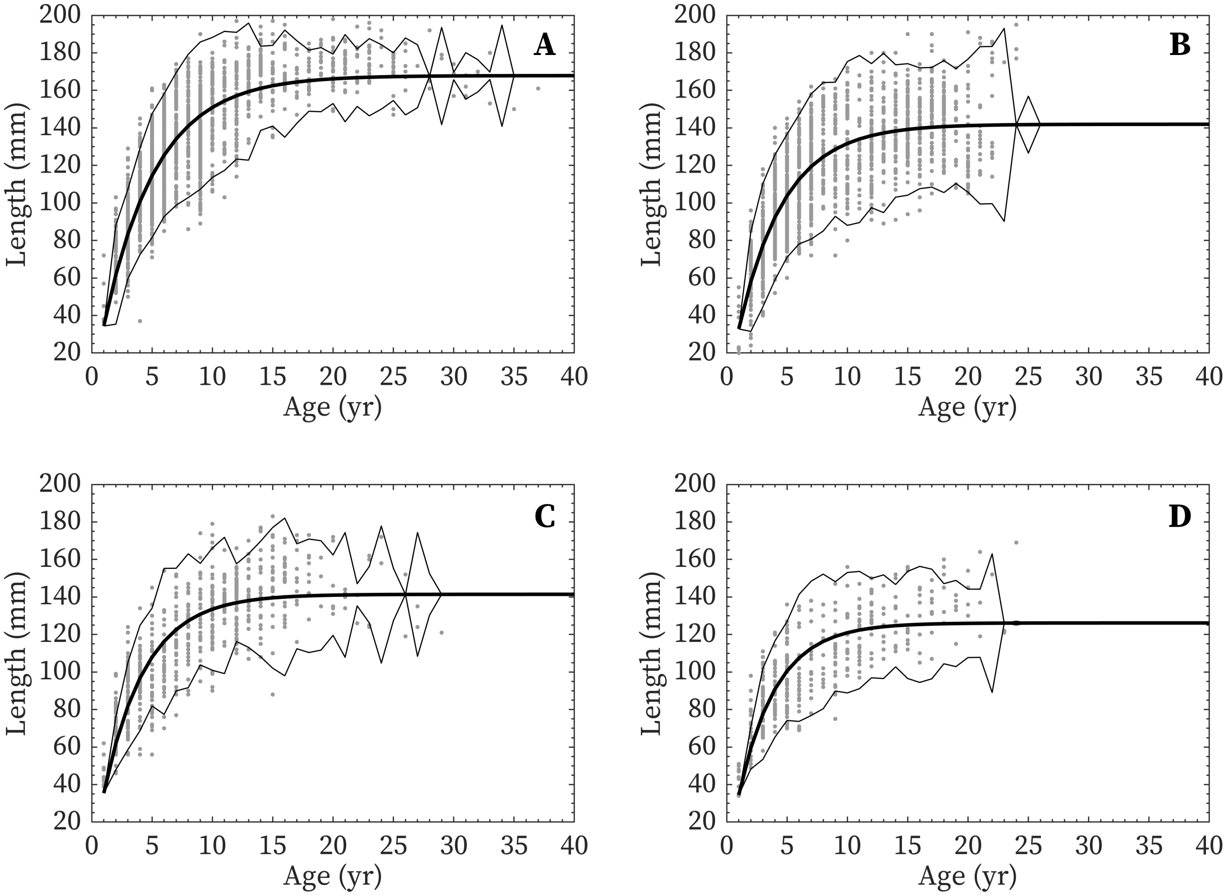

Figure A.2. Atlantic surfclam age (yr) versus length (mm) observations (grey dots) obtained from the Delmarva Peninsula survey region for (A) 1980s, (B) 1990s, (C) 2000s, and (D) 2010s. The growth curve (heavy line) and standard deviation (2σ, thin line) obtained from the von Bertalanffy equation fit to the observations for each decade is shown. All curve fits are significant ($p < 0.001$) with r^2 values of 0.71 for the 1980s, 0.62 for the 1990s, 0.72 for the 2000s and 0.61 for the 2010s.

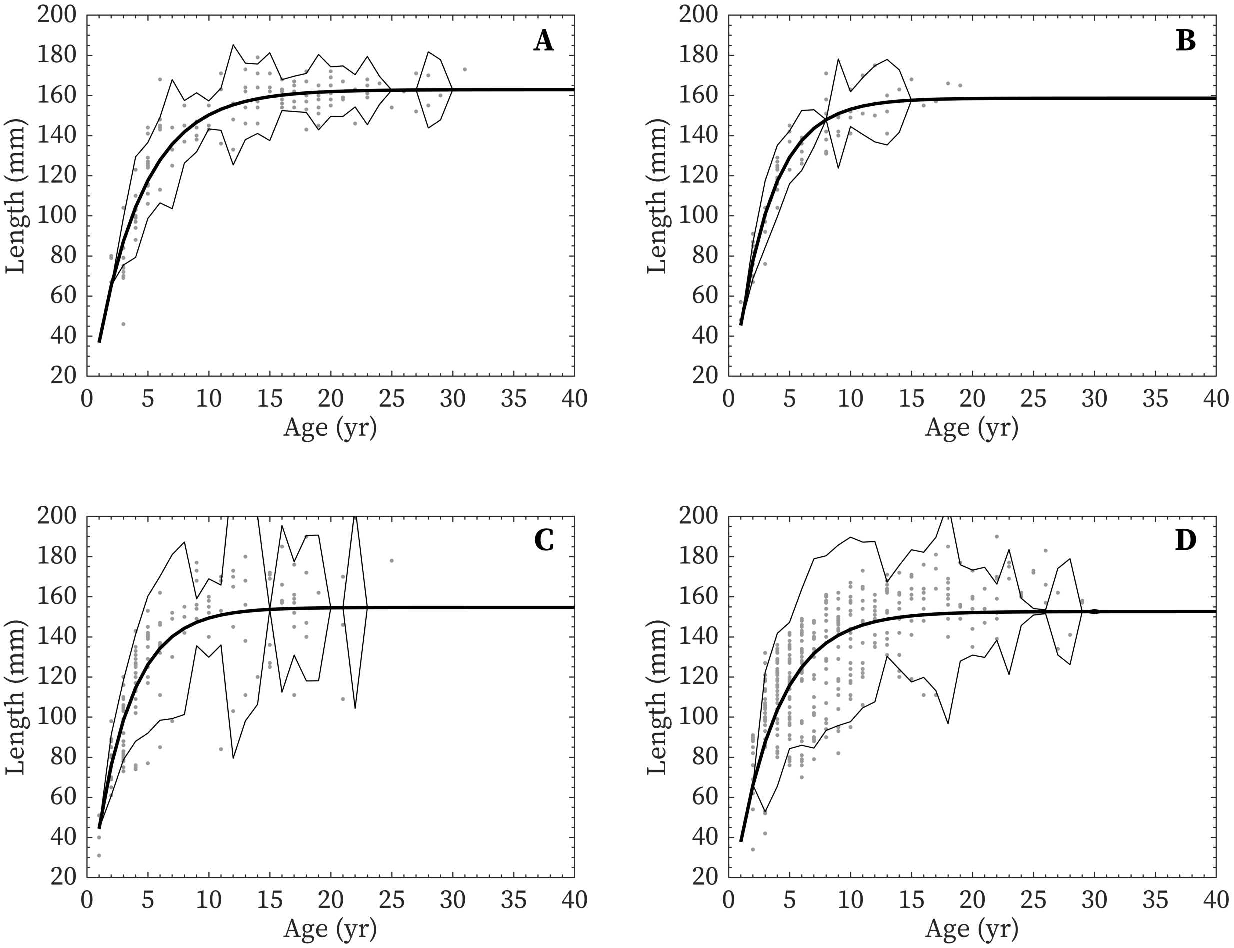

Figure A.3. Atlantic surfclam age (yr) versus length (mm) observations (grey dots) obtained from the Long Island survey region for (A) 1980s, (B) 1990s, (C) 2000s, and (D) 2010s. The growth curve (heavy line) and standard deviation (2σ, thin line) obtained from the von Bertalanffy equation fit to the observations for each decade is shown. All curve fits are significant ($p < 0.001$) with r^2 values of 0.87 for the 1980s, 0.90 for the 1990s, 0.69 for the 2000s and 0.50 for the 2010s.

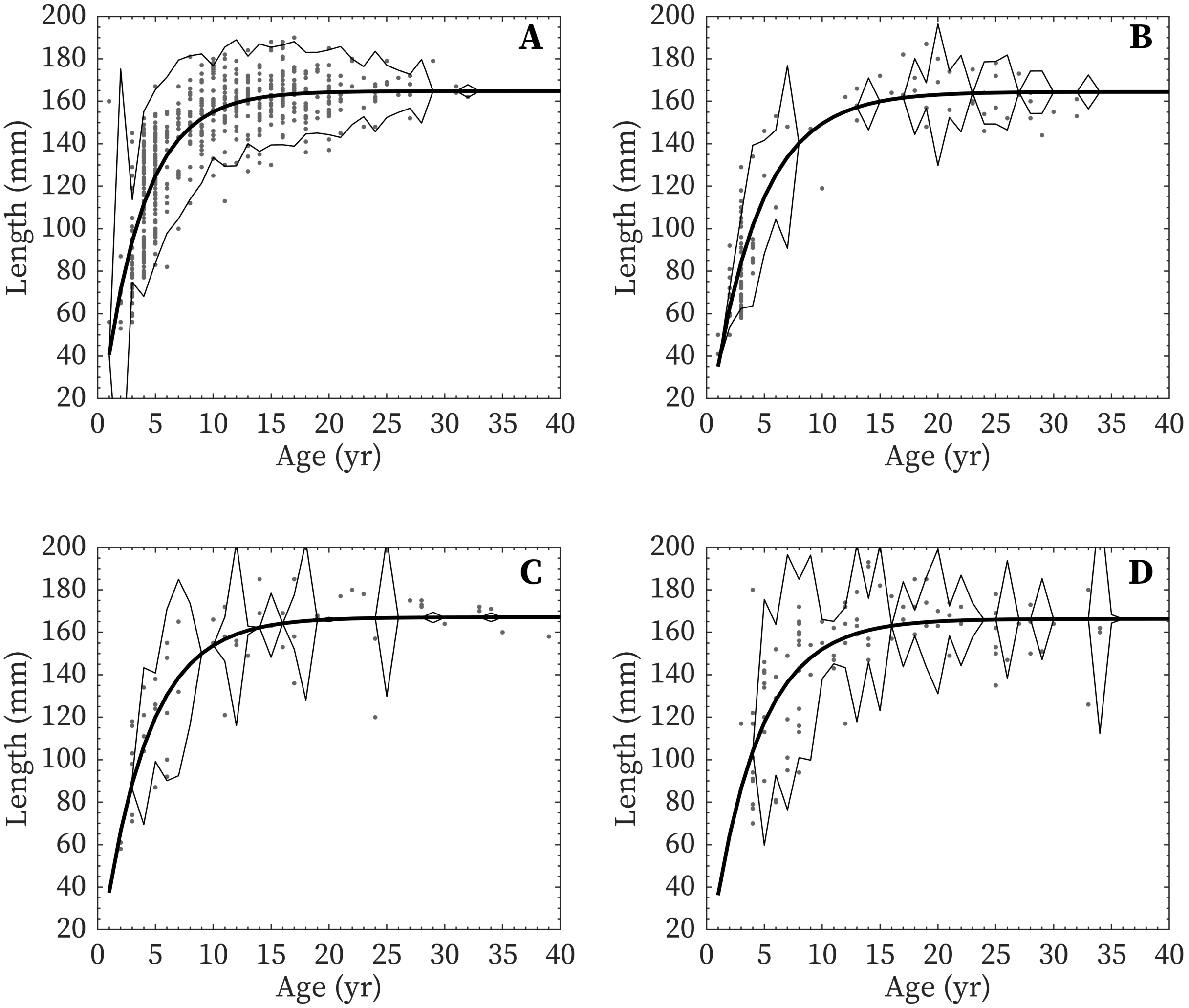

Figure A.4. Atlantic surfclam age (yr) versus length (mm) observations (grey dots) obtained from the Southern New England survey region for (A) 1980s, (B) 1990s, (C) 2000s, and (D) 2010s. The growth curve (heavy line) and standard deviation (2σ, thin line) obtained from the von Bertalanffy equation fit to the observations for each decade is shown. All curve fits are significant ($p < 0.001$) with r^2 values of 0.70 for the 1980s, 0.87 for the 1990s, 0.77 for the 2000s and 0.51 for the 2010s.

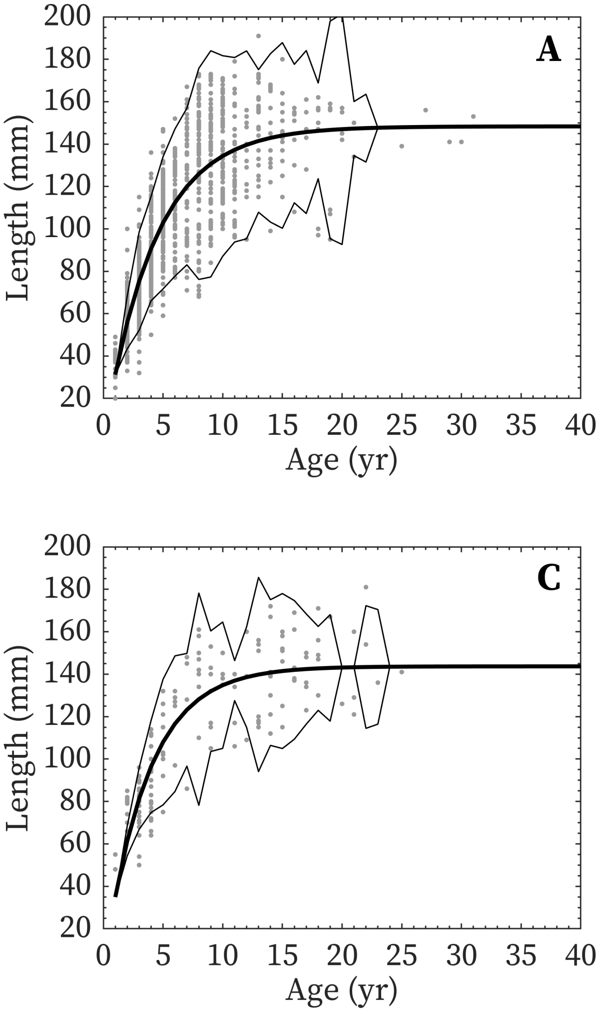

Figure A.5. Atlantic surfclam age (yr) versus length (mm) observations (grey dots) obtained from the Georges Bank survey region for (A) 1980s, (B) 1990s, (C) 2000s, and (D) 2010s. The growth curve (heavy line) and standard deviation (2σ, thin line) obtained from the von Bertalanffy equation fit to the observations for each decade is shown. All curve fits are significant ($p < 0.001$) with r^2 values of 0.72 for the 1980s, 0.71 for the 1990s, 0.74 for the 2000s and 0.59 for the 2010s.

VON BERTALANFFY PARAMETERS

TABLE B.1.

Summary statistics for fitting of the von Bertalanffy equation (Equation 1) to the Atlantic surfclam age and length observations from each survey region for each decade. The resulting specific growth rate (k, yr^{-1}) and asymptotic length (L_∞, mm) are shown. The explained variance of the fit of Equation (1) to the observation is indicated by the regression coefficient, r^2. The F-value, F, and degree of freedom, *df*, are shown for each regression. Survey regions are defined as: SVA-Southern Virginia, DMV-Delmarva Peninsula, NJ-New Jersey, LI-Long Island, SNE-Southern New England, GBK-Georges Bank.

Survey Region	Decade	k	L_∞	r^2	F	df
SVA	1980s	0.34	152.13	0.66	4880	183
	1990s	0.38	143.38	0.84	216	6
	2000s	0.38	131.45	0.84	494	27
	2010s	0.67	104.93	0.56	1750	68
DMV	1980s	0.22	167.87	0.71	59500	2087
	1990s	0.26	141.94	0.62	30400	1558
	2000s	0.29	141.42	0.72	24100	984
	2010s	0.32	126.16	0.61	8130	383
NJ	1980s	0.27	165.02	0.74	128000	3724
	1990s	0.26	158.82	0.75	54300	1466
	2000s	0.26	155.28	0.62	37300	1863
	2010s	0.26	149.30	0.65	31900	1149
LI	1980s	0.26	162.89	0.87	9860	124
	1990s	0.34	158.63	0.90	6850	67
	2000s	0.34	154.66	0.69	6180	269
	2010s	0.28	152.62	0.50	7450	371
SNE	1980s	0.28	164.81	0.70	23100	620
	1990s	0.24	164.44	0.87	3190	102
	2000s	0.25	167.09	0.77	3900	96
	2010s	0.25	166.35	0.51	2440	97
GBK	1980s	0.24	148.33	0.72	18200	1109
	1990s	0.27	146.41	0.71	10600	537
	2000s	0.28	143.67	0.74	6870	262
	2010s	0.29	148.96	0.59	21300	640

AGE-DEPENDENT MORTALITY FIGURES

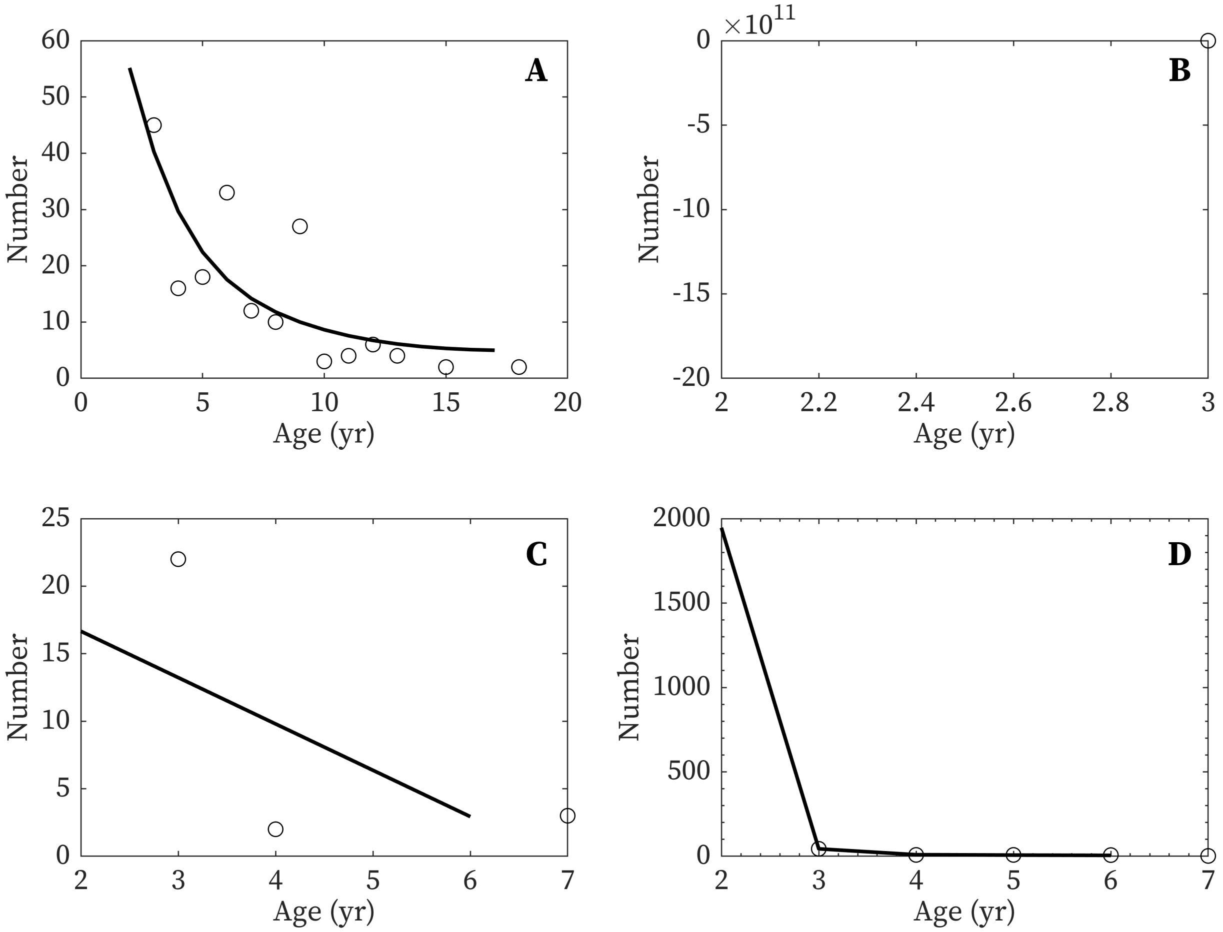

Figure C.1. Age (yr) versus number of Atlantic surfclam observations in each age category (circles) obtained from the stock surveys in the Southern Virginia region for (A) 1980s, (B) 1990s, (C) 2000s, and (D) 2010s. The mortality curve (solid line) obtained from the fit of equation (4) is shown.

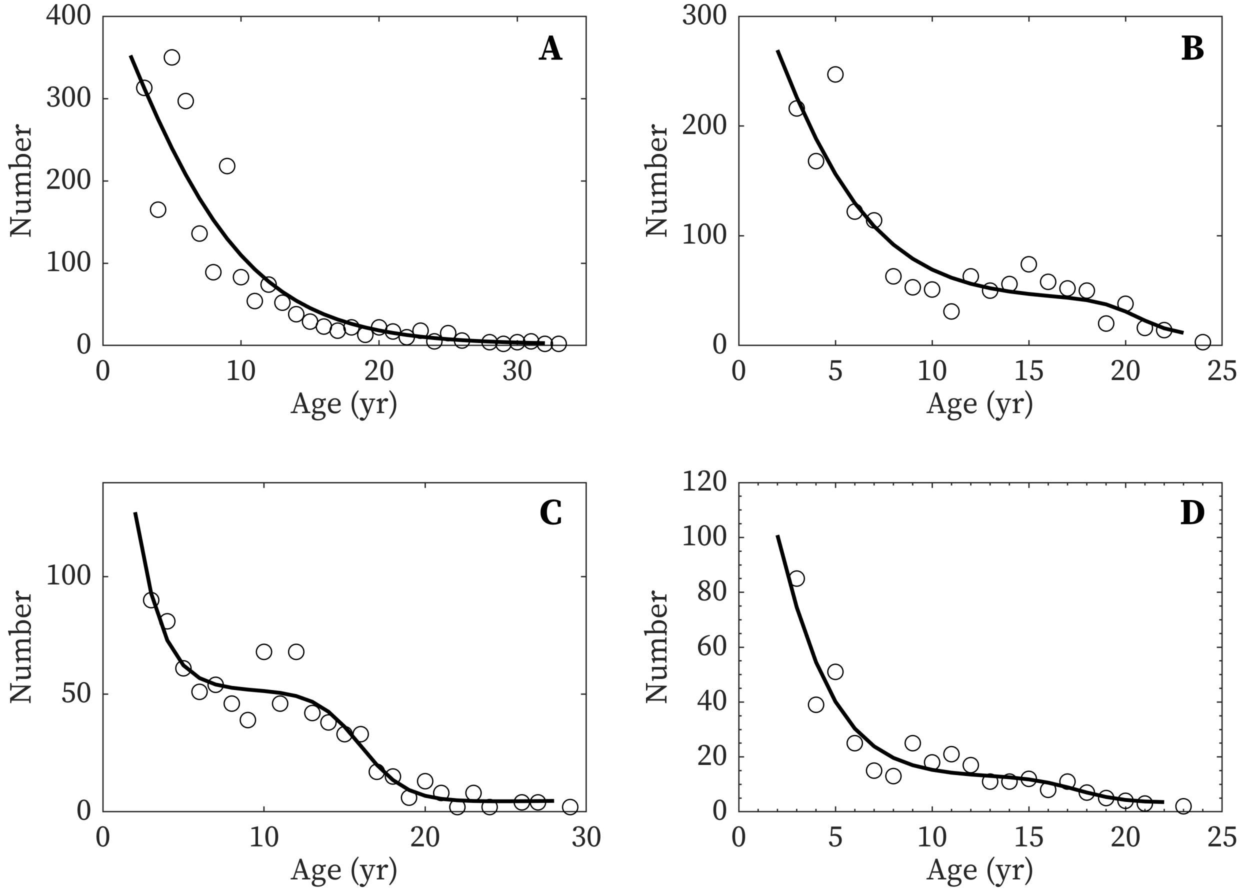

Figure C.2. Age (yr) versus number of Atlantic surfclam observations in each age category (circles) obtained from the stock surveys in the Delmarva Peninsula region for (A) 1980s, (B) 1990s, (C) 2000s, and (D) 2010s. The mortality curve (solid line) obtained from the fit of equation (4) is shown. All curve fits are significant ($p < 0.001$) with r^2 values of 0.81 for the 1980s, 0.78 for the 1990s, 0.91 for the 2000s and 0.85 for the 2010s.

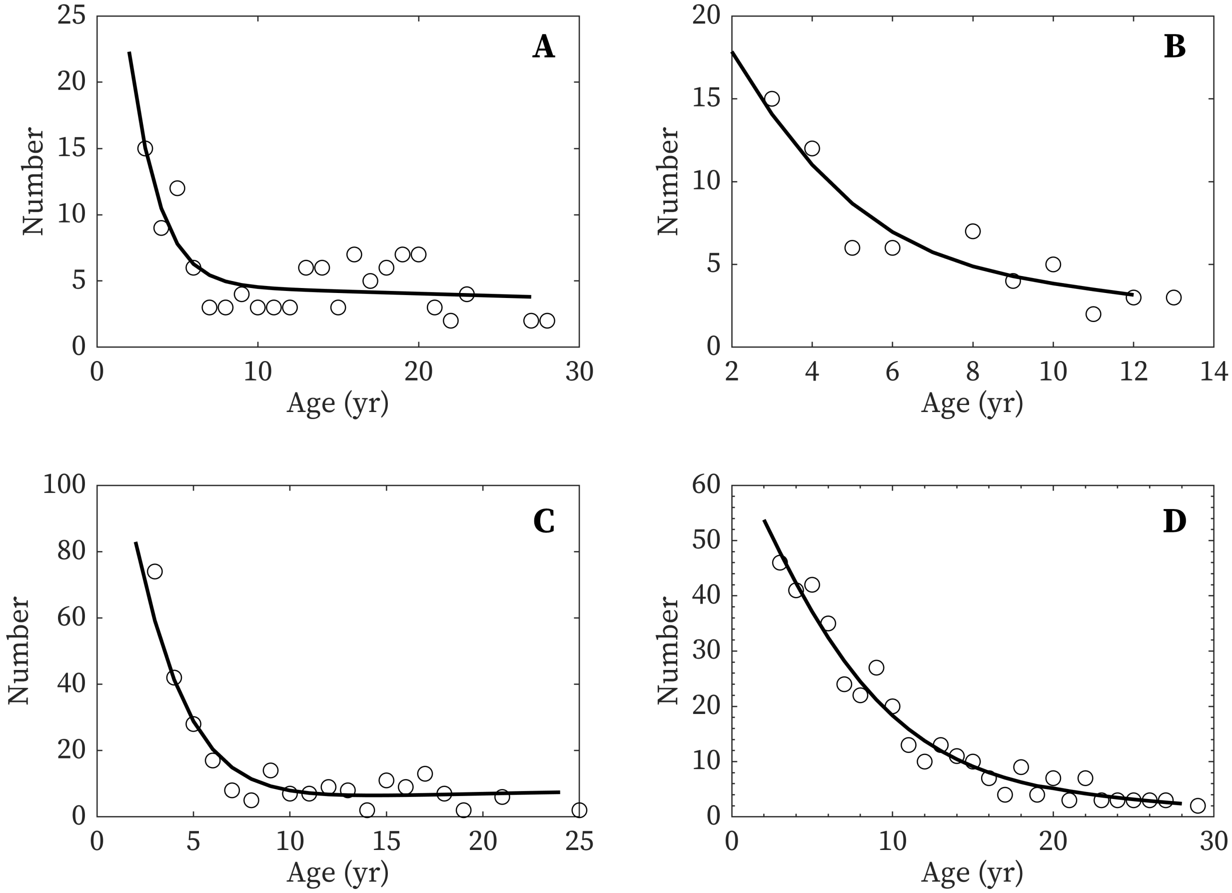

Figure C.3. Age (yr) versus number of Atlantic surfclam observations in each age category (circles) obtained from the stock surveys in the Long Island for (A) 1980s, (B) 1990s, (C) 2000s, and (D) 2010s. The mortality curve (solid line) obtained from the fit of equation (4) is shown. All curve fits are significant ($p < 0.001$) with r^2 values of 0.58 for the 1980s, 0.65 for the 1990s, 0.86 for the 2000s and 0.96 for the 2010s.

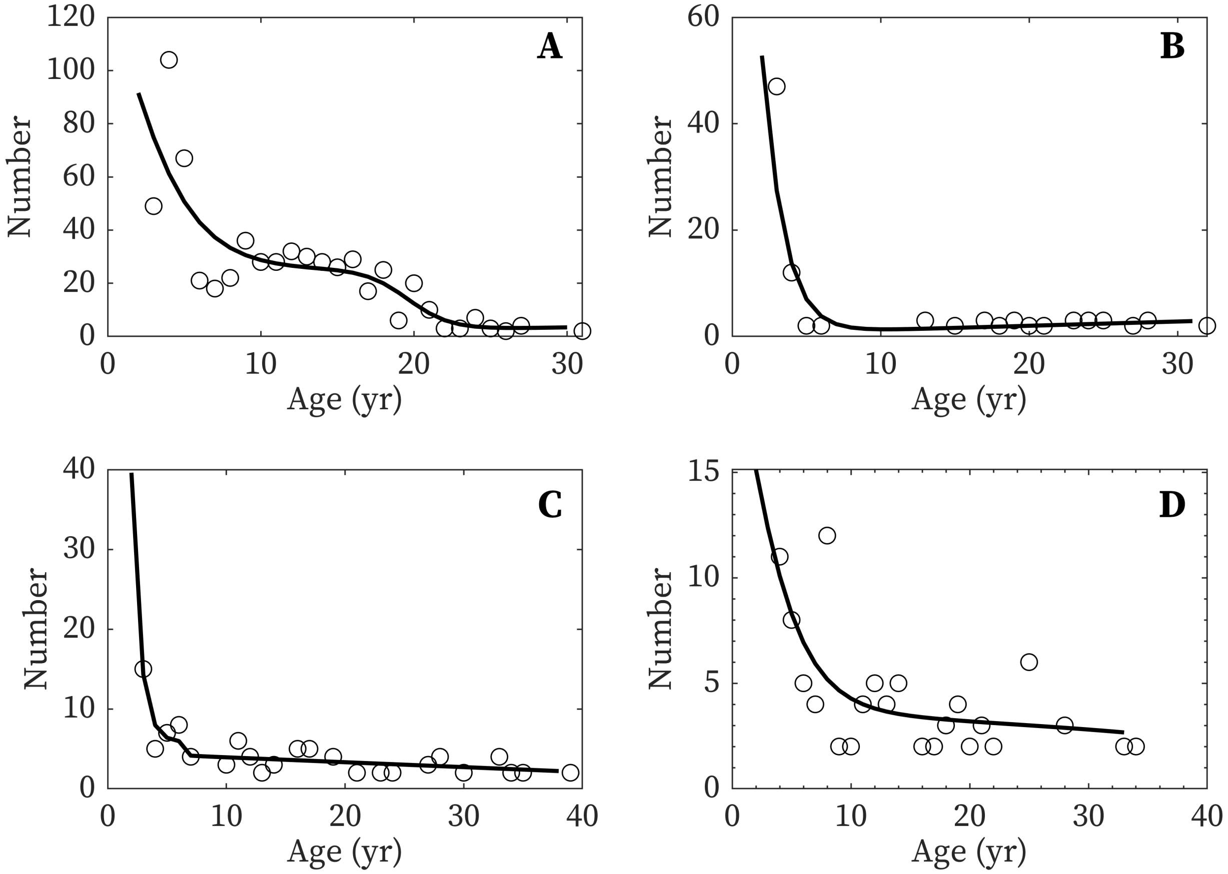

Figure C.4. Age (yr) versus number of Atlantic surfclam observations in each age category (circles) obtained from the stock surveys in the Southern New England for (A) 1980s, (B) 1990s, (C) 2000s, and (D) 2010s. The mortality curve (solid line) obtained from the fit of equation (4) is shown. All curve fits are significant ($p < 0.001$) with r^2 values of 0.58 for the 1980s, 0.72 for the 1990s, 0.77 for the 2000s and 0.28 for the 2010s.

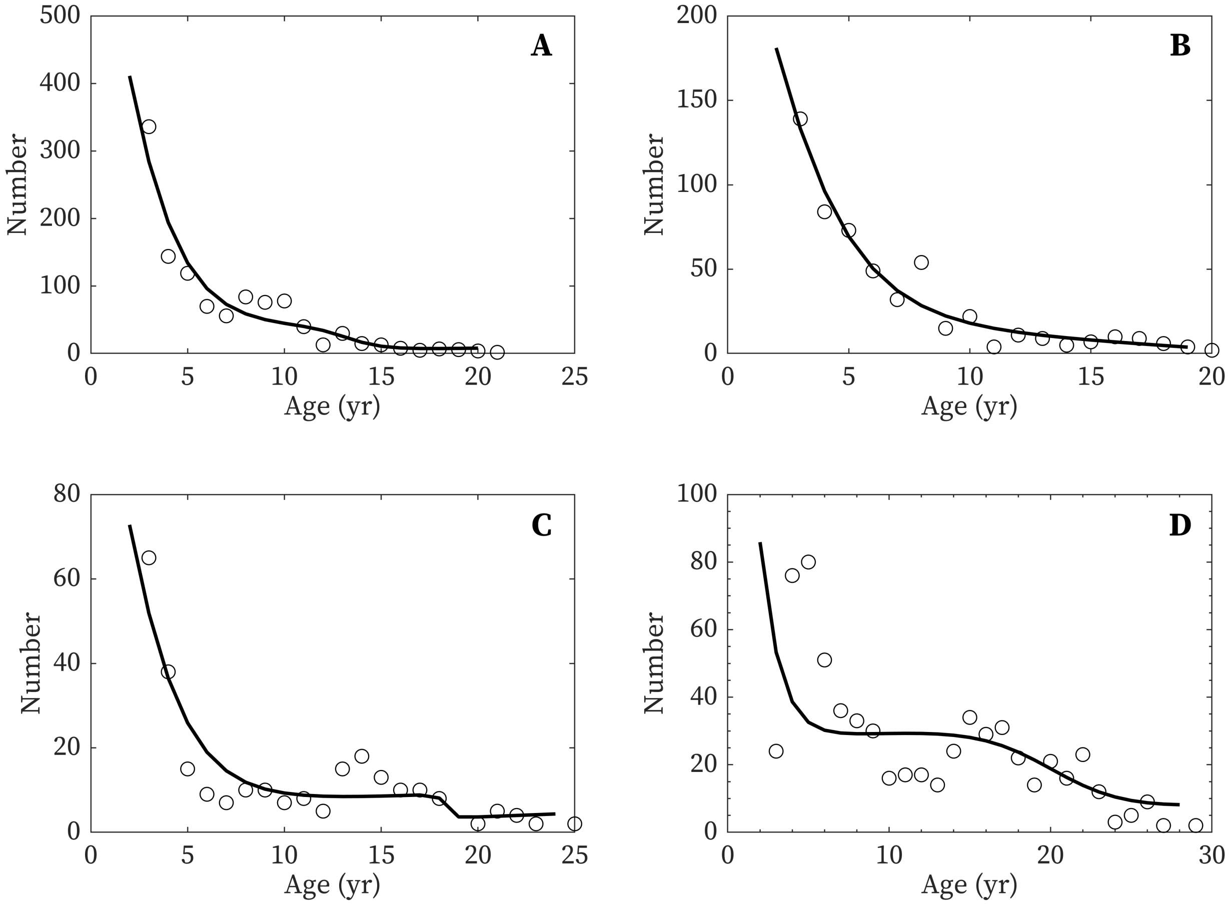

Figure C.5. Age (yr) versus number of Atlantic surfclam observations in each age category (circles) obtained from the stock surveys in the Georges Bank for (A) 1980s, (B) 1990s, (C) 2000s, and (D) 2010s. The mortality curve (solid line) obtained from the fit of equation (4) is shown. All curve fits are significant ($p < 0.001$) with r^2 values of 0.88 for the 1980s, 0.94 for the 1990s, 0.79 for the 2000s and 0.16 for the 2010s.

AGE-DEPENDENT MORTALITY PARAMETERS

TABLE D.1.
Summary statistics from fitting of Equation (4) to the Atlantic surfclam age and length observations from each survey region for each decade. The coefficient values shown in columns 3 to 10 are defined in section *Mortality Rate*. The explained variance of the fit of Equation (4) to the observations is indicated by the regression coefficient, r^2. Summary statistics for fitting of the von Bertalanffy equation (Equation 1) to the Atlantic surfclam age and length observations from each survey region for each decade. The resulting specific growth rate (k, yr^{-1}) and asymptotic length (L_∞, mm) are shown. The explained variance of the fit of Equation (1) to the observation is indicated by the regression coefficient, r^2. The F-value, F, and degree of freedom, df, are shown for each regression. Survey regions are defined as: SVA-Southern Virginia, DMV-Delmarva Peninsula, NJ-New Jersey, LI-Long Island, SNE-Southern New England, GBK-Georges Bank.

Survey Region	Decade	N_0	N_1	a_1	dN_1	a_{max}	a_m	a_r	M_{base}	r^2	F	df
SVA	1980s	–	–	–	–	–	–	–	–	–	–	–
	1990s	–	–	–	–	–	–	–	–	–	–	–
	2000s	–	–	–	–	–	–	–	–	–	–	–
	2010s	–	–	–	–	–	–	–	–	–	–	–
DMV	1980s	397.99	37.99	10.30	0.00	0.09	0.05	0.10	0.03	0.81	41.8	26
	1990s	365.23	35.20	6.62	0.00	0.01	20.66	2.10	0.32	0.78	28.3	14
	2000s	246.77	50.95	2.82	-0.12	-20.51	16.01	2.86	0.08	0.91	98.3	18
	2010s	168.44	10.77	4.34	0.00	-0.05	17.48	2.66	0.14	0.85	33.7	13
NJ	1980s	982.10	36.86	9.20	0.36	43.85	18.46	1.84	-0.38	0.93	83.8	27
	1990s	550.85	81.85	3.44	0.55	92.04	20.96	1.76	-1.89	0.95	147	18
	2000s	428.06	30.71	6.49	0.00	0.00	25.43	2.11	0.38	0.87	53.9	22
	2010s	197.81	20.83	8.18	0.00	0.03	25.92	2.26	0.07	0.85	55.6	24
LI	1980s	44.95	4.75	3.15	0.01	0.64	93.83	2.21	-0.04	0.58	11.4	19
	1990s	26.97	1.89	5.09	0.00	0.01	12.98	3.23	0.12	0.65	12.7	3
	2000s	144.74	3.93	4.22	0.00	0.05	34.47	8.12	0.16	0.86	30.6	12
	2010s	66.35	6.09	9.80	0.25	23.93	19.52	-0.05	-0.15	0.96	264	21
SNE	1980s	131.80	23.40	5.10	0.00	0.01	19.60	2.79	0.11	0.58	15.5	19
	1990s	147.87	0.40	2.60	2.78	459.23	49.30	0.69	0.08	0.72	15.2	13
	2000s	321.00	6.22	1.40	0.13	34.39	6.52	0.026	-0.06	0.77	19	18
	2010s	21.67	3.81	5.26	0.00	0.01	55.86	13.56	-0.03	0.28	11.6	15
GBK	1980s	760.15	34.50	3.80	0.00	0.00	13.19	1.88	0.40	0.88	31	12
	1990s	302.45	21.45	4.40	0.45	44.78	19.97	0.09	-0.93	0.94	88.7	13
	2000s	128.40	5.71	4.06	0.00	0.00	18.33	0.39	0.18	0.79	23.2	14
	2010s	237.422	26.95	2.19	0.00	0.00	20.05	4.67	0.26	0.16	8.6	19

SIMULATED ATLANTIC SURFCLAM POPULATION TIME EVOLUTION

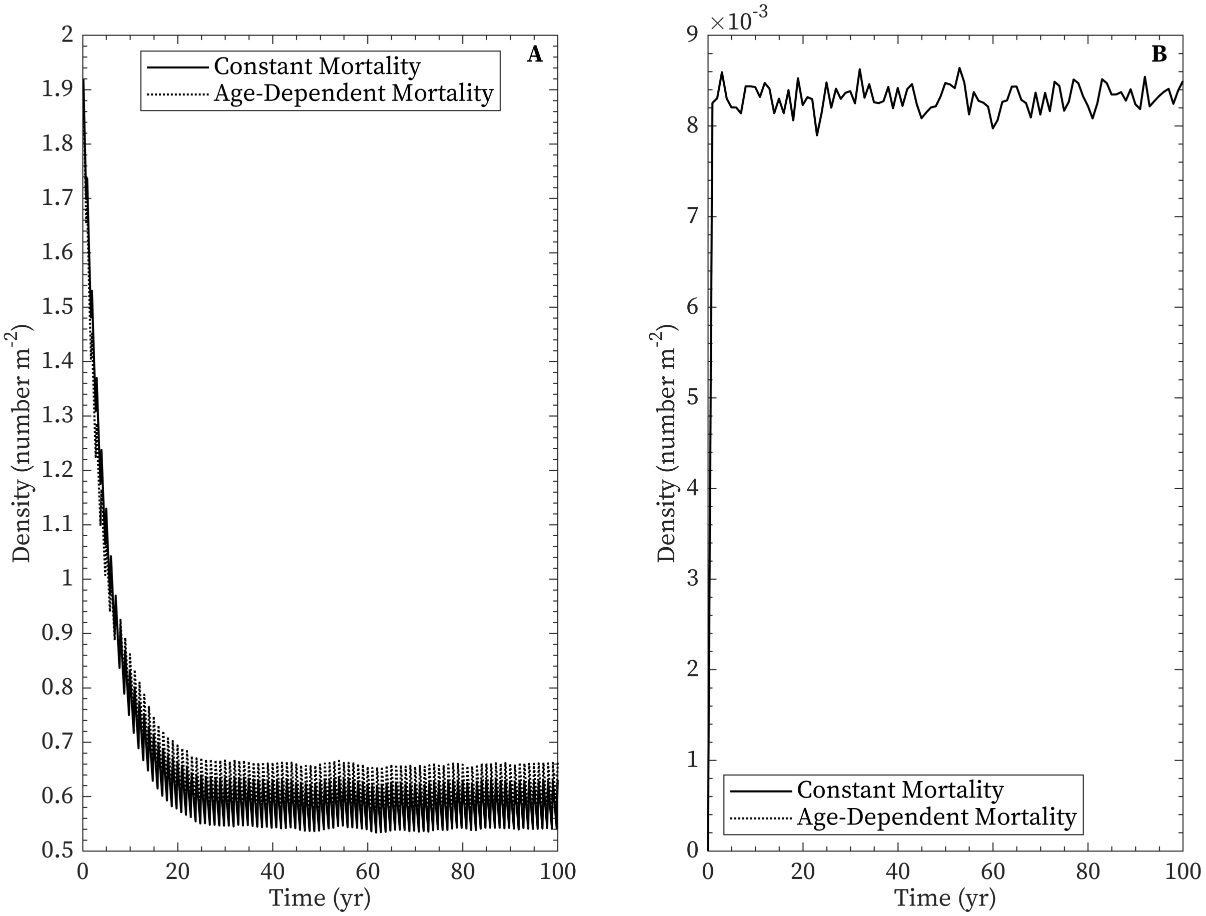

Figure E.1. Simulated time evolution for Atlantic surfclam (A) reproductive clam density and (B) recruit density for the 1990s.

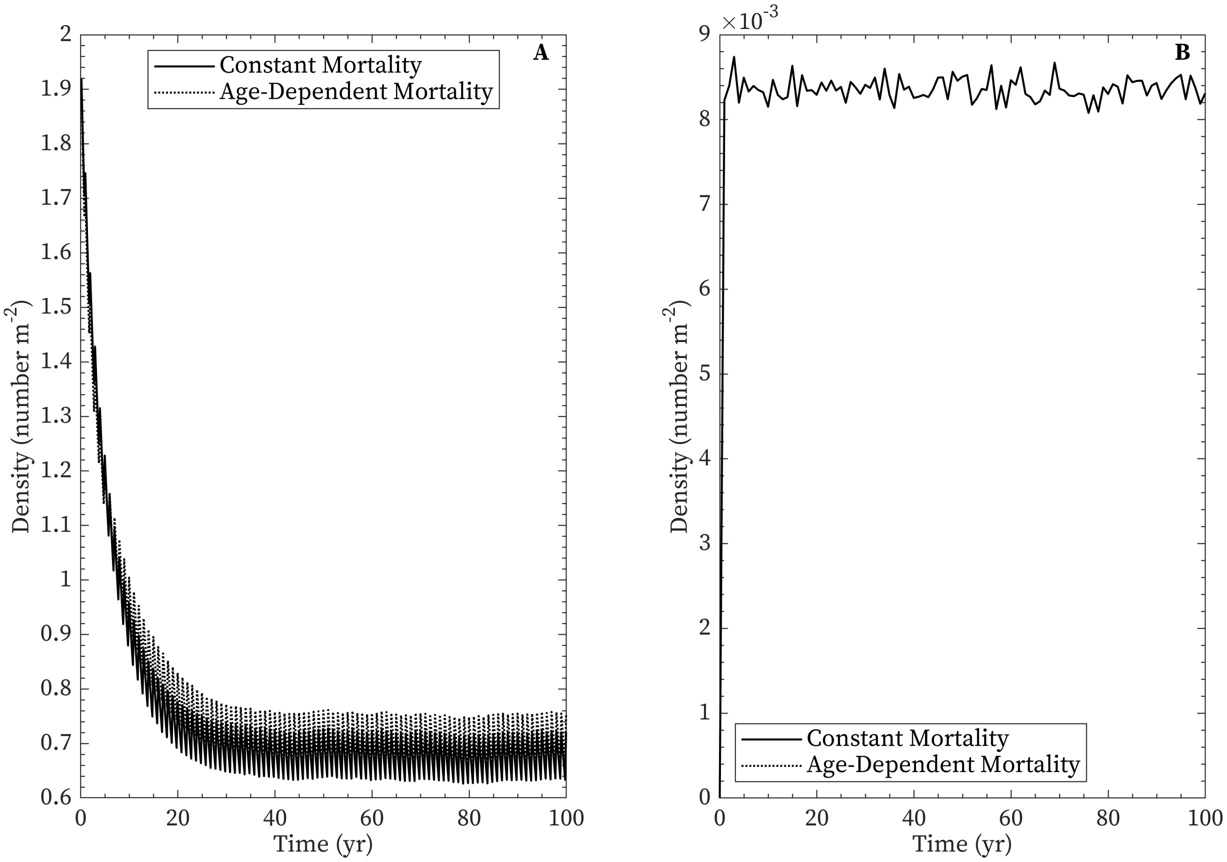

Figure E.2. Simulated time evolution for Atlantic surfclam (A) reproductive clam density and (B) recruit density for the 2000s.

VITA

Mauricio González Díaz
Department of Ocean and Earth Sciences
Old Dominion University
Norfolk, VA, 23529

EDUCATION
2022 (*expected*) — M.S. Ocean and Earth Sciences, Old Dominion University
2019 — B.S. Marine Biology, Universidad Austral de Chile, Chile

AWARDS AND NOMINATIONS
2022 — Nomination Outstanding Graduate Teaching Assistant (Laboratory Instructor)
2020 — Dorothy Brown Smith Travel Scholarship (*Cancelled due to COVID-19*)

EMPLOYMENT
2022 — Teaching Assistant Introductory Meteorology — Old Dominion University
2019–2022 — Teaching Assistant Introductory Oceanography — Old Dominion University
2018–2019 — Zooplankton and Data Analyst — Centro IDEAL, Universidad Austral de Chile

PUBLICATIONS AND PRESENTATIONS
2021, November — Coastal and Estuarine Research Federation: 26th Biennial Conference
2021, March — National Shellfisheries Association: 113th Annual Conference
2020, December — AGU Fall Meeting
2020, November — American Fisheries Society 150th Annual Meeting
2018, May — 38th Chilean Ocean Sciences Conference

PROFESSIONAL SOCIETIES
American Geophysical Union
Coastal and Estuarine Research Federation
The Oceanography Society

CONTACT
Email — maugondiaz@gmail.com

Typesetting using LaTeX